Facies Architecture, Paleo-hydraulics and Fluvial Style of a Falling Stage Terrace Deposit within a Compound Incised Valley System, Ferron Notom Delta, Utah

---

A Thesis
Presented To
the Faculty of the Department of Earth and Atmospheric Sciences,
University of Houston

In Partial Fulfillment of
the Requirements for the Degree of
MASTERS IN SCIENCE

By
Cameron R. Griffin
May, 2013

Facies Architecture, Paleo-hydraulics and Fluvial Style of a Falling Stage Terrace Deposit within a Compound Incised Valley System, Ferron Notom Delta, Utah

_____

Cameron R. Griffin

APPROVED:

_____

Dr. Janok P. Bhattacharya, Advisor

_____

Dr. William Dupre, Committee Member

_____

Dr. Mark Barton, Committee Member

_____

Dean, College of Natural Sciences and Mathematics

ACKNOWLEDGEMENTS

First and foremost, I would like to thank my loving wife for her unending support and encouragement while writing this thesis. So often, she has put aside her own career goals and aspirations so that I can reach mine. For these reasons, I dedicate this thesis to her. I would also like to recognize and thank my family, especially my mother and father, for their love and support and for all that they have done in helping me to reach this point in my life.

I would especially like to recognize and thank my advisor, Dr. Janok P. Bhattacharya, for his tireless help, guidance, and support in writing this thesis. I came to the University of Houston to study under his tutelage and am grateful for his vast knowledge and enthusiasm for geology. His patience, guidance, and direction in the field, in the classroom and individually has been greatly appreciated and has allowed me to write this work.

I would also like to extend my gratitude to Dr. Mark Barton and Dr. William Dupre for serving on my committee and providing me with important experience and ideas in writing this thesis. My appreciation goes out to Benjamin Hilton, Chris Campbell, Omar Montes, Danfix D'Souza, Ben Browning, Mohammad Ullah, Chenliang Wu, JianQiao Wang, Oyebode Fambode, and Yang Yang Li who provided me with encouragement, critique and intellectual discussion throughout the research and writing of this thesis. I am especially grateful to Chris Campbell and Benjamin Hilton for their collaboration and support. Additionally, I would like to thank all those involved with the

funding of the QSL Consortium which includes: Exxon Mobil, Shell, Nexen, BP, EcoPetrol, Inpex, Pioneer, BHP Billiton, Chevron, and Anadarko.

Facies Architecture, Paleo-hydraulics and Fluvial Style of a Falling Stage Terrace Deposit within a Compound Incised Valley System, Ferron Notom Delta, Utah

---

An Abstract for a Thesis
Presented To
the Faculty of the Department of Earth and Atmospheric Sciences,
University of Houston

In Partial Fulfillment of
the Requirements for the Degree of
MASTERS IN SCIENCE

By
Cameron R. Griffin
May, 2013

FACIES ARCHITECTURE, PALEO-HYDRAULICS AND FLUVIAL STYLE OF A FALLING STAGE TERRACE DEPOSIT WITHIN A COMPOUND INCISED VALLEY SYSTEM, FERRON NOTOM DELTA, UTAH

ABSTRACT

Incised valley systems are important because they contain significant hydrocarbon reserves, provide clues into the geologic history of a region, and are crucial for sequence stratigraphic interpretations. The fluvial/deltaic Notom Delta component of the Turonian (Late Cretaceous) Ferron Sandstone Member of the Mancos Shale outcrops in south-central Utah providing an excellent opportunity to study a terrace deposit in both strike and dip orientations of a compound incised valley system. Using traditional field methods conducted during the summer of 2012, detailed cross sections and bedding diagrams were created that show a terrace deposit (Valley 3) that has been previously undescribed. This terrace deposit formed in response to multiple sea-level fluctuations. The presence of a tidal signature along with the proximity of the incised valley system to the coastal plain (parasequence 4) suggest the presence of a Coastal Plain Valley System. Fill from this incised valley deposit would also fall within the shorter, less preserved deposits of the segment 2 middle incised valley deposits of the idealized longitudinal incised valley model. Paleocurrent and bar accretion measurements taken from within individual channel belts of the incised valley generally showed accretion occurring at high angles to that of the paleocurrent direction. This suggests the fluvial style responsible for the formation of this incised valley system was

meandering. Previous regional stratigraphic studies have shown that the incised valley system within the study area is a falling stage terrace deposit. This is incongruous with previous sequence stratigraphic models that early, falling stage valley fills are a result of braided rivers. Paleo-flow depths that were calculated based on cross-set thicknesses for Valley 3 indicate an average flow depth of 3.3 to 5.4 meters.

TABLE OF CONTENTS

LIST OF FIGURES

LIST OF TABLES

SECTION 1. OVERVIEW

1.1 Introduction

Incised valley systems, along with their preserved deposits, are known to contain significant hydrocarbon reserves and may host approximately 25% of all off-structure conventional petroleum traps in clastic reservoirs (Boyd et al., 2006). For this reason, understanding the internal organization and facies architecture of incised valley systems is important for determining the reservoir geometry, connectivity, and fluid flow of analog reservoirs associated with incised valley systems.

Studies on outcrops of incised valleys in the ancient help understand the architecture of incised valley fill and improve existing models for incised valleys. Three-D seismic may be ideal in determining larger scale complexities associated with incised valleys but are unable to detect finer scale facies variations. Well logs and cores, on the other hand, are excellent for recognizing smaller scale vertical variations but are difficult for predicting lateral variations. Therefore, a high volume of outcrop exposure in both dip and strike views may be the best way to document and understand incised valley fills. This information will potentially be valuable in helping to determine the size, shape, and interconnectivity of sand bodies associated with incised valleys. More detailed work is needed to determine, in detail, the fill heterogeneity of incised valley deposits. This information will be useful for evaluating the economic potential of valley systems as a reservoir and for improving current models of incised valleys.

In addition to their economic significance, incised valleys also provide important clues about the stratigraphic history of the region in which they are found (Ardies et al., 2002; Strong & Paola, 2008; Martin et al., 2011). Understanding the fluvial architecture of incised valley fill deposits can provide important insights into global sea level changes, climate, fluvial style, and shifts in depositional environments (Zaitlin et al., 1994; Ardies et al., 2002; Wellner & Bartek, 2003; Boyd et al., 2006; Gibling, 2006). Incised valley systems also play an important role in sequence stratigraphic interpretations, as the base and sides of the valley signify an unconformity and, as such, represent an important criterion for the identification of sequence boundaries (Dalrymple et al., 1994).

Incised valley systems can be filled with a complex array of depositional systems that include open marine to estuarine to fluvial environments (Zaitlin et al., 1994; Posamentier 2001). Therefore, current incised valley models often oversimplify their complex nature (fig. 1.1A) (Boyd et al. 2006). The Notom Delta of the Ferron Sandstone outcrops along Neilson Wash providing an opportunity to study the 3D facies heterogeneity of a compound incised valley deposits and its associated fill (fig. 1.1A). This study aims to identify and describe the bedding architecture of a terrace deposit within a compound incised valley system and also to estimate the paleo-hydraulics of the river system that occupied it.

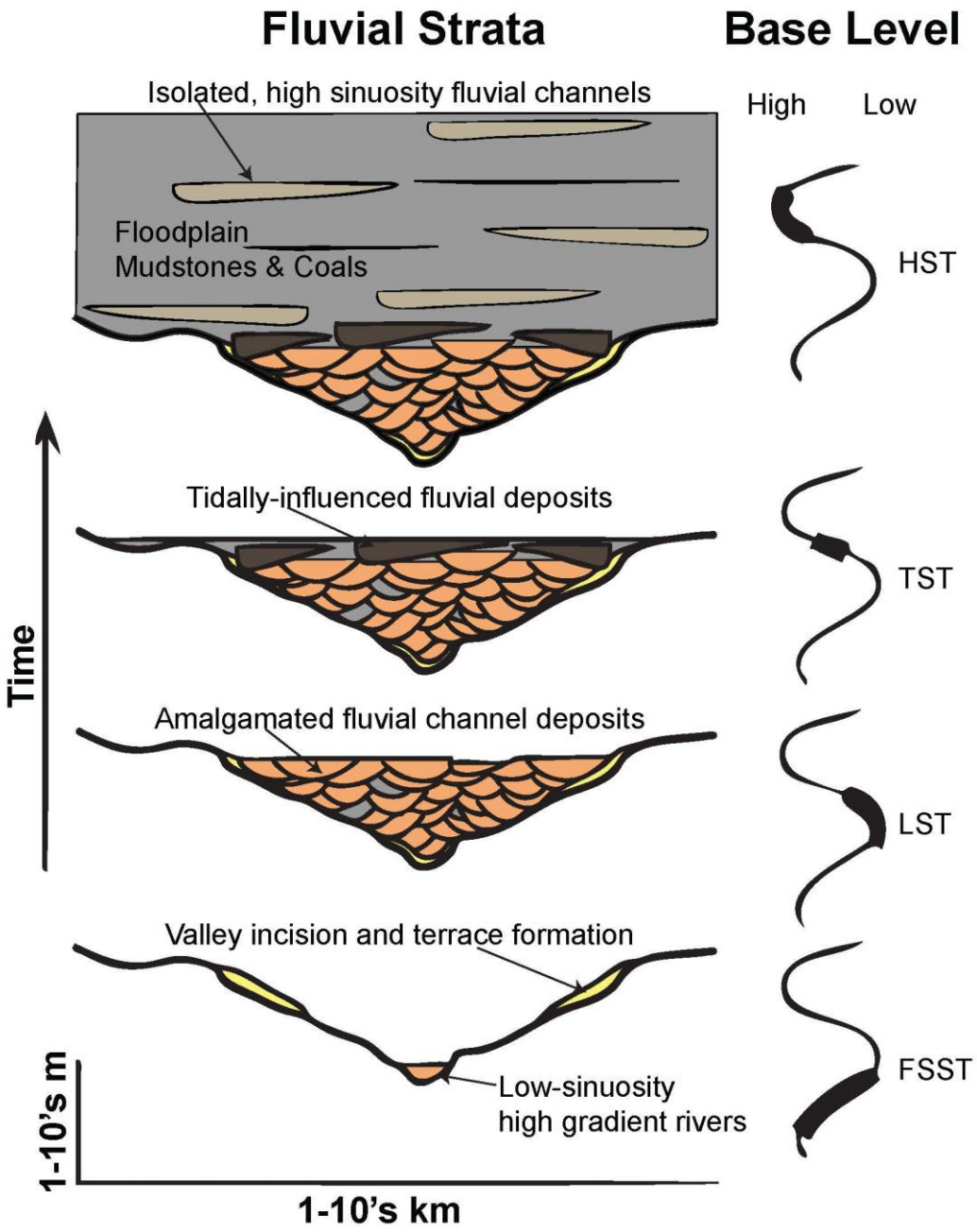

Figure 1. An idealized strike section of a simple incised valley system that predicts fill type as a function of base level rise. This model predicts muddier facies and/or increase in tidally influenced facies and lessening degrees of confinement within the valley as gradients decrease. Figure unmodified from Hilton, 2013, who modified it from Shanley and McCabe, 1994.

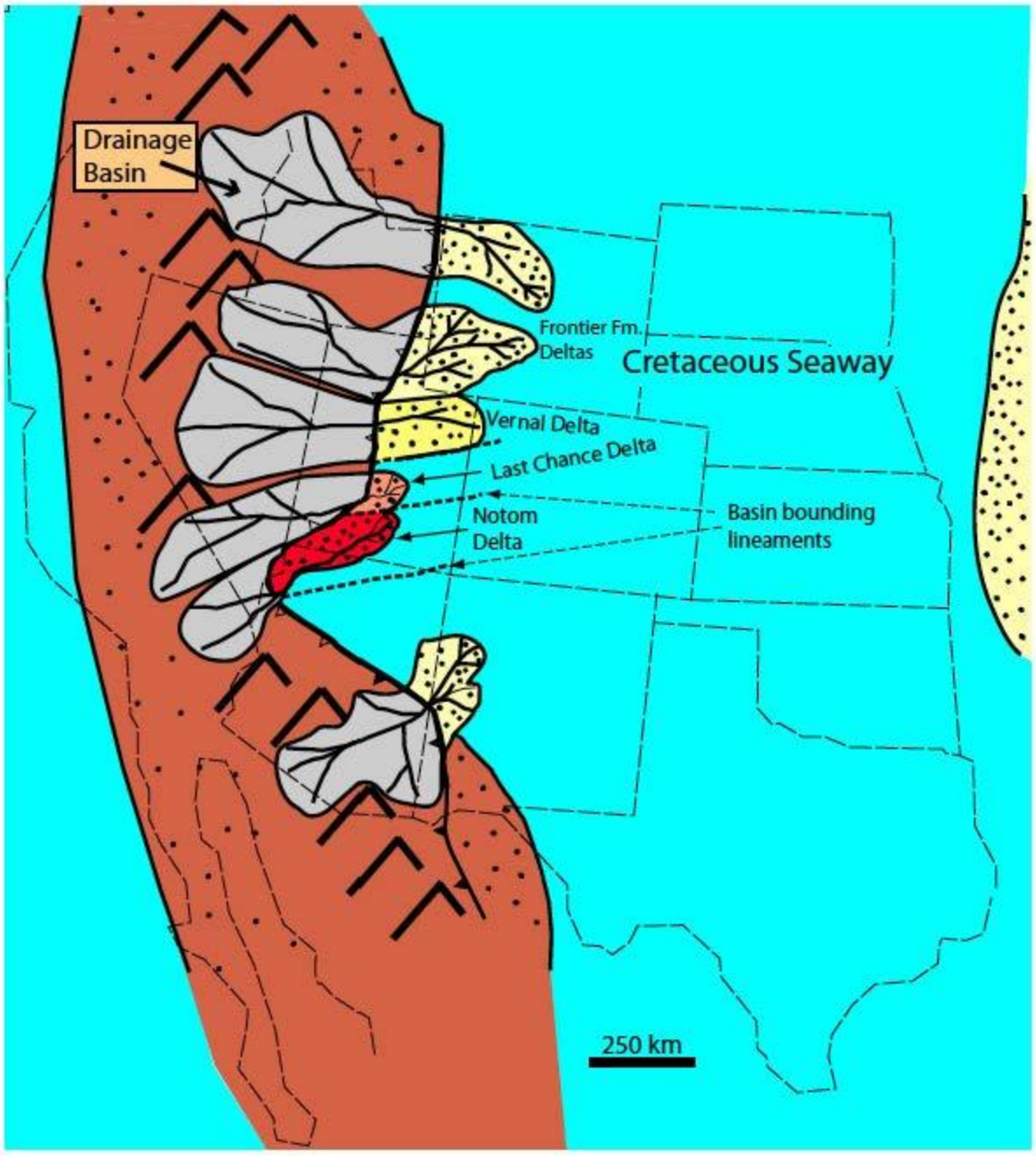

Figure 2. Paleogeographic map of the Cretaceous western margin of North America. Illustrates the major depocenters associated with the Ferron Sandstone (from Bhattacharya & Tye, 2004; based on Gardner, 1995).

1.2 Incised Valley Systems

Posamentier (2001) described incised valleys as occurring where a river has eroded deep enough into its own floodplain so that even when the river is in its flood stages, it does not overtop the riverbanks. Incised valley systems, which include both the incised valley and its depositional fill, are defined by Zaitlin et al., 1994 as a "fluvially-eroded, elongate topographic low that is typically larger than a single channel form, and is characterized by an abrupt seaward shift of depositional facies across a regionally mappable sequence boundary at its base." Zaitlin et al., (1994) also provided a generalized, strike-oriented cross section through an incised valley system in an estuarine, wave-dominated environment (fig. 1.2A). Shanley and McCabe (1994) have predicted depositional fill patterns within a simple incised valley system as a function of base-level changes (fig. 2).

Zaitlin et al. (1994) identified several key elements for the recognition of incised valleys in outcrop. Some of these key elements include: an abrupt basinward shift in facies across a sharp erosional contact that can be traced up onto an interfluve for some distance, and stratal truncation and onlap. However, identifying an incised valley based solely on these criteria can be very difficult. In order to aid in the recognition of incised valleys, Bhattacharya and Tye (2004) have developed a quantitative method to distinguish incised valleys from single channels based on the comparison between total depth of incision and calculated bankfull water depth.

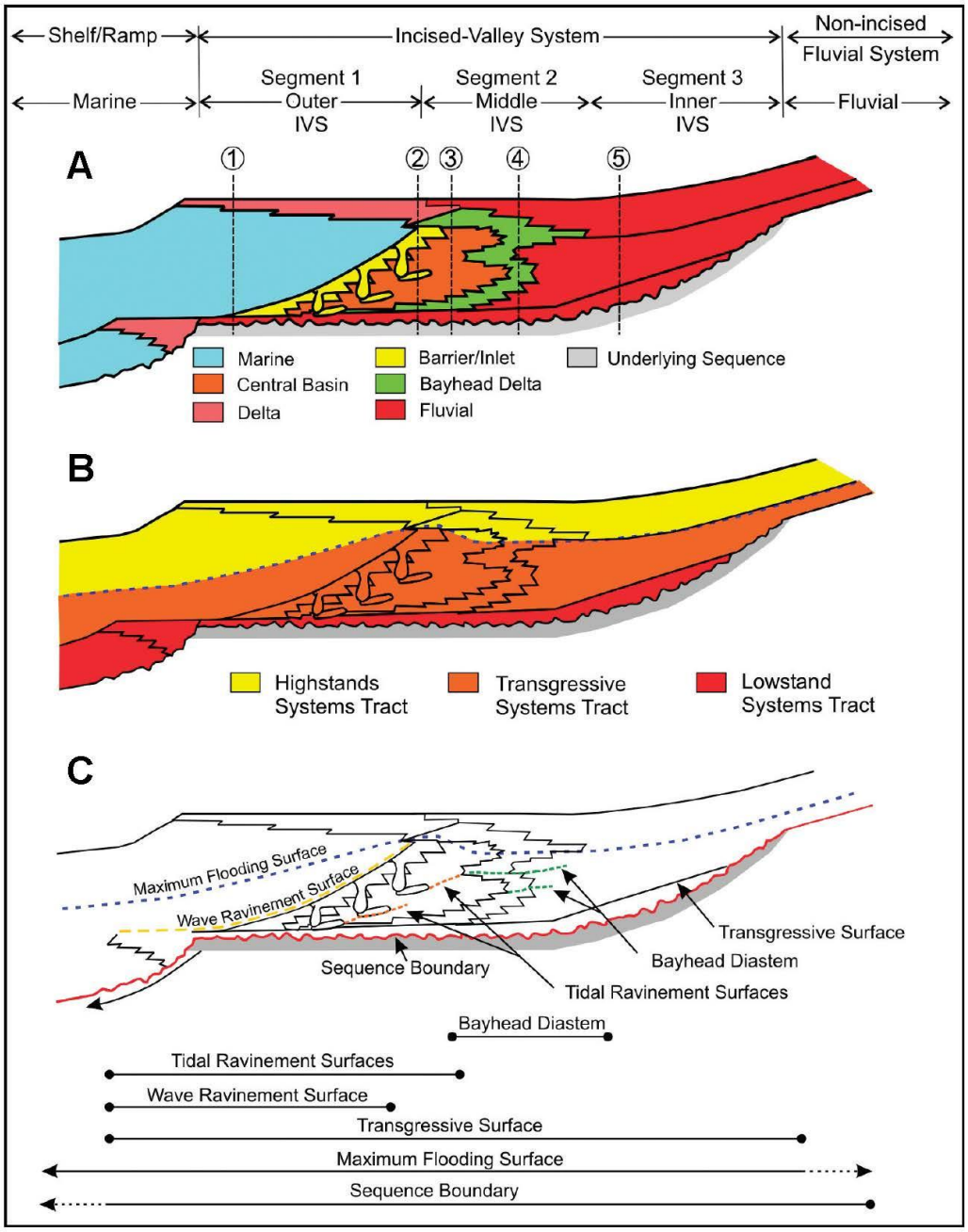

Figure 3. A generalized longitudinal cross section through an incised valley system in a wave-dominate estuarine environment. Figure illustrates probable depositional environments, distribution of systems tracts and key stratigraphic surfaces. Figure from Zaitlin et al., 1994.

Incised valleys typically occur in response to a variety of variables. Some of the more important variables include: sea-level fluctuations, tectonics, and climate (Posamentier, 2001), which drive base-level fluctuations and sediment supply and discharge (Shanley & McCabe, 1994; Holbrook et al., 2006). Changes in base level cause changes in both stream slope and velocity, which, in turn, determine whether the fluvial morphology will be straight, braided, or meandering (Zaitlin et al., 1994; Bridge, 2006). Systems tracts have also been identified based on the fluvial architecture of valley fills and their relationship to shoreface stacking patterns as a function of base level (fig. 2) (Shanley and McCabe, 1994). The purpose of this study is to examine complex incised valleys within the Cretaceous Ferron Sandstone along Neilson Wash. The main objectives of this study will be: 1. to extend previous research in the area 2. describe a terrace deposit that has previousely been unrecognized and 3. Determine the paleo-hydraulics and fluvial morphology of the river that occupied the terrace deposit.

1.3 Regional Geology

The Turonian Ferron Sandstone Member of the Cretaceous Mancos Shale is made up of several fluvial-deltaic wedges associated with the Cretaceous Western Interior Seaway (fig. 2) (Bhattacharya and Tye, 2004). These clastic wedges formed in response to an increase in accommodation resulting from the subsidence of the retroarc foreland basin east of the ancestral Rocky Mountains (Peterson and Ryer, 1975; Gardner, 1995; Garrison & van den Bergh, 2004; Zhu et al., 2012). The Ferron Sandstone Member of the Mancos Shale Formation is bounded below by a gradational contact with

the Tununk Shale. The Ferron is then capped with an erosive contact by the Blue Gate Shale (fig. 4) (Garrison & Van Den Bergh, 2004).

The Ferron Sandstone is composed of sediments derived from the Sevier Orogeny to the west and was deposited during a "greenhouse" period in which Utah was located at approximately 45˚N to 50˚N (Ryer & Anderson, 2004; Gibling, 2006). Immature gleysols and abundant coals within the Ferron indicate that the climate during the time of deposition was humid and subtropical (Bhattacharya & Tye, 2004). At its height, the Western Interior Seaway connected the Gulf of Mexico to the Northern Boreal Sea (Fig. 2) (Plint & Wadsworth, 2003; Bhattacharya & MacEachern, 2009; Zhu et al, 2012). The Ferron itself has been divided into two different lithostratographic units (Garrison & Van Den Bergh, 2004). The upper portion of the Ferron Sandstone is considered to be predominantly fluvial in nature while the lower Ferron is composed of shallow marine deposits (Peterson & Ryder, 1975; Ryer & Anderson, 2004).

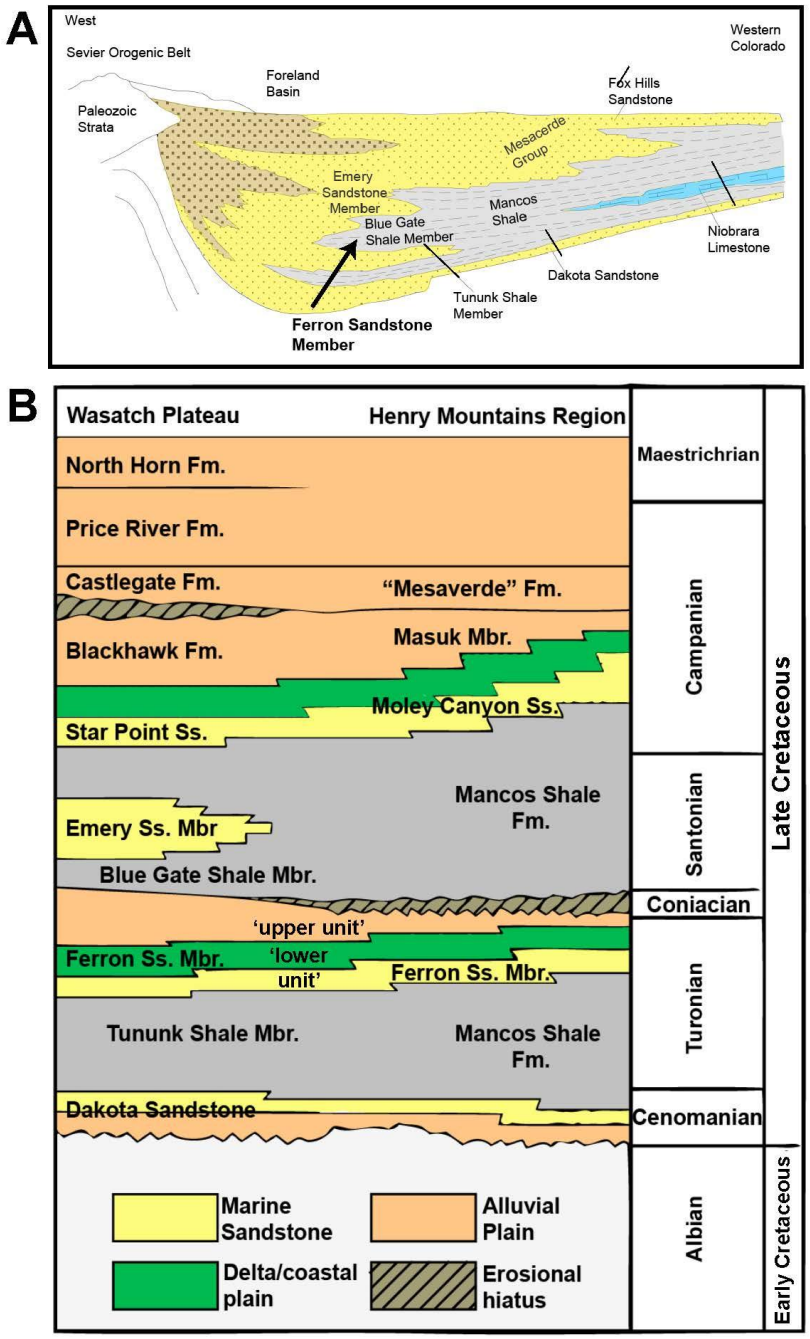

Figure 4. Cretaceous wedge showing the stratigraphic position of the Ferron Sandstone along with a stratigraphic column for the Henry Mountain Basin. Figure from Hilton, in prep., who modified it from Peterson and Ryder, 1975; and Peterson et al., 1980.

The Ferron Sandstone is composed of several different clastic wedges (fig. 2). The most well-known and well-studied of these wedges is known as the Last Chance Delta (Chidsey et al., 2004). However, comparatively less focus has been placed on the Notom Delta, which contains excellent exposure just north of the Henry Mountains in Southern Utah (fig. 5). $^{40}Ar/^{39}Ar$ age dates from sanidine crystals found in bentonite beds throughout the Notom Delta indicate that the delta prograded into the seaway approximately 91.25 ± 0.77 Ma ago (Zhu et al., 2012). Radiometric age calculations also showed that the Notom Delta was deposited over a period of approximately 620,000 years. This gives an approximate time span of 100,000 years for the deposition of each sequence (Zhu, 2010; Zhu et al., 2012). This relatively high frequency of depositional cycles is hypothesized to reflect in part, global ice level variations that are associated with Milankovitch Cycles (Li et al., 2010; Zhu et al, 2012; Campbell, 2013).

1.4 Previous Work

The compound incised valley system being considered for this study is located in the Notom Delta in Southern Utah. Outcrop and measured sections were taken in modern day Neilson Wash, which is located approximately 16 kilometers west of Hanksville, UT along Coal Mine Road (fig. 5). Previous studies by Zhu et al. (2010) and Li et al. (2010) have shown that the Notom Delta is composed of 43 parasequences that are grouped into 18 parasequence sets (fig. 6) (Zhu et al., 2012). These parasequences sets can be grouped into 6 depositional sequences, which display degradational, progradational, aggradational, and retrogradational stacking patterns (Zhu et al., 2012).

The focus of this study will be on the incised valleys from sequence 1 that erode into the marine sandstones and shales of sequence 2 (fig. 5).

Campbell (2013) and Li et al. (2010) have done extensive previous work on the IVS in Neilson Wash along the eastern cliff face (fig. 5). Li et al. (2010) conducted a detailed study on the facies architecture and facies relationships of outcrop areas stretching from just south of the Fremont River up through Neilson Wash. Initially, Li et al. (2010) subdivided the IVS into two different valley fill sequences (V1 and V2) bounded by regionally traceable erosional surfaces that exhibit an anomalous juxtaposition of proximal fluvial sandstone on top of more distal marine facies (fig. 7). However, one of the aims of this study is to both show and describe an older valley fill sequence that demonstrates the same attributes as those described previously. In order to maintain the same nomenclature designation as provided by Li et al. (2010), this new valley has been labeled as V3. The resulting nomenclature for the IVS found in Neilson Wash, listed from oldest to youngest is V3, V2, and V1. Accordingly, younger valley fills and surfaces are designated a suffix letter in descending order indicating increasingly younger deposits. Therefore, valley sequences and valley allomembers would be labeled from oldest to youngest as V3B, V3A, V2B, V2A and SB1c, Sb1b, Sb1a respectively (Hilton, 2013). This nomenclature method also matches work done by Campbell (2013) and Hilton (2013) in order to ensure consistency.

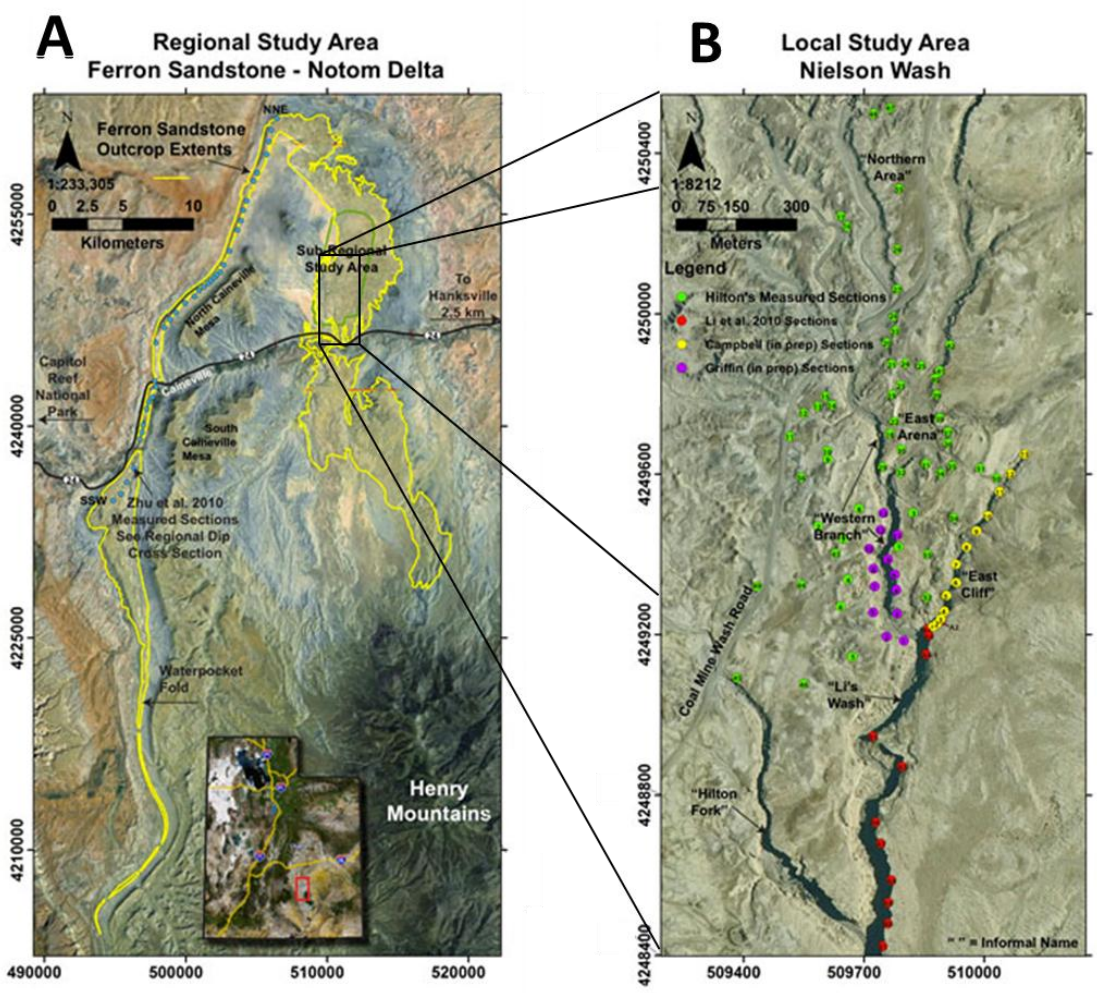

Figure 5. A) Satellite imagery showing the Ferron Notom Delta (delineated with yellow lines) in Southern Utah. B) Satellite imagery of the study area located with Neilson Wash. Purple circles represent measured sections taken for this study during the summer of 2012. Yellow, green and red circles represent measured sections taken by Campbell (2013), Hilton (2013) and Li et al (2010) respectively. The projected horizontal datum used for these maps is WGS 1984, UTM Zone 12N. Figure modified from Hilton, 2013.

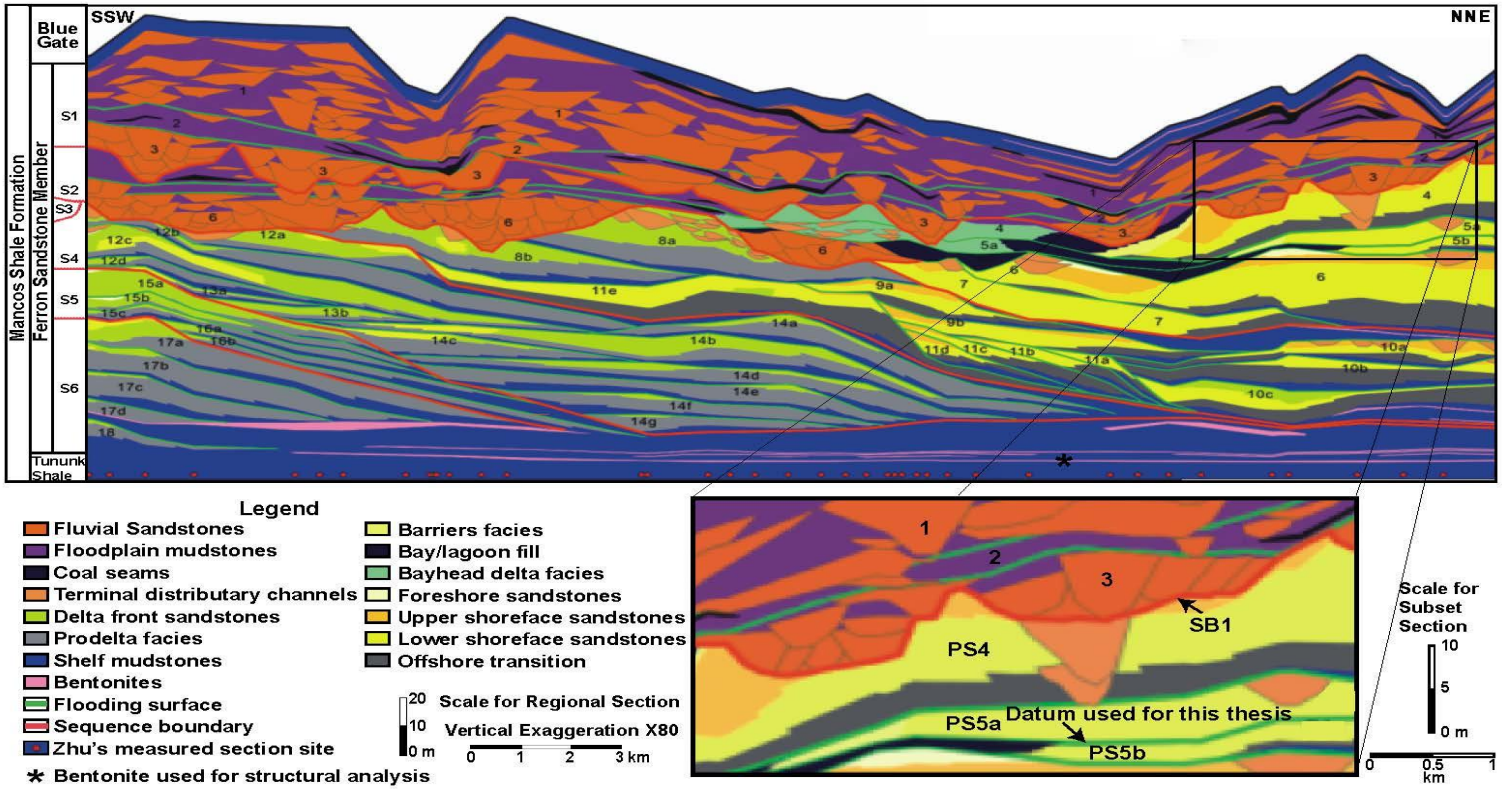

Figure 6. A dip section of the Ferron Notom Delta showing 6 sequences, 18 parasequence sets, and 43 parasequences that were deposited over 620,000 years. The zoomed region of the section demonstrates the stratigraphic relationships of sequence 1 fluvial strata eroding into sequence 2 marine strata that are found within the study area. The incised valley shown within the zoomed region may not be the same valley segments that are feeding the incised valleys within the study area. The source feeding the Neilson Wash study area is unkown but may be one of the 3 incised valleys in sequence 1 located to the left of the image. Figure modified from Hilton, 2013, who modified it after Zhu et al., 2012.

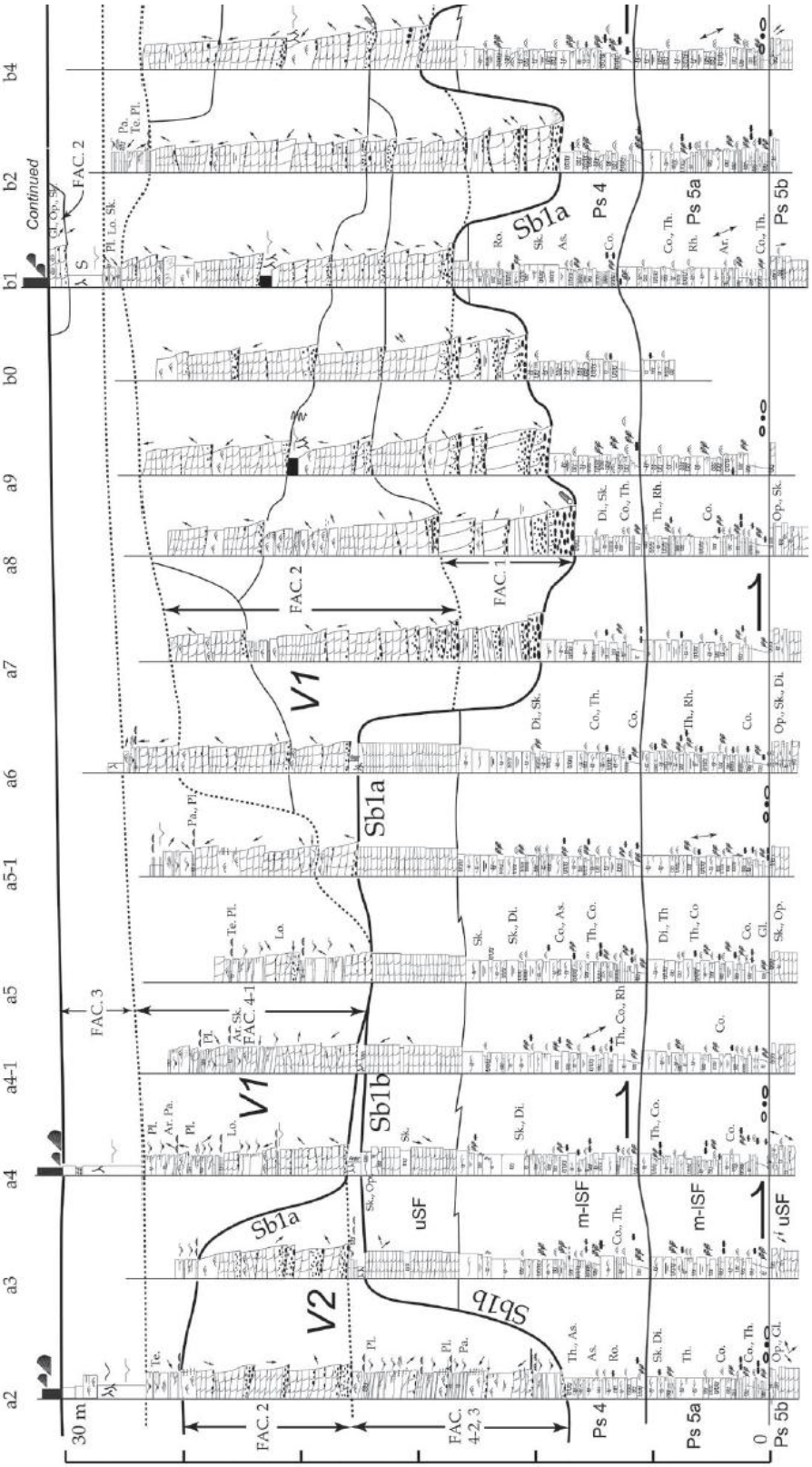

Figure 7. Figure showing measured sections made by Li et al. (2010) along the eastern cliff face of Neilson wash. Measured sections taken along the western cliff face of Neilson wash will be correlated to previous work done by Li et la., (2010) and Campbell (2013).

SECTION 2. METHODS AND FACIES DESCRIPTIONS

2.1 Methods

In order to map the incised valley system, a total of 13 measured sections were taken in Neilson Wash during the summer of 2012. The thesis area is located along the northern end of Neilson Wash where there is a junction between two branches of the wash (Fig. 8). This junction allows for a view of the IVS in both strike and dip orientations. Measured sections were taken along the western branch of the wash (Fig. 8). Data for this thesis were taken in the form of measured sections that record both grain size and sedimentary structure. Digital photographs, photomosaics, lidar images, paleocurrent directions, and cross-set thickness measurements were also taken and used to aid with interpretation and mapping. Equipment that was used to collect this data include: a hand lens, metric tape measure, grain size card, Garmin handheld GPS, Jacob's Staff, and Brunton Compass. Figures and photographs were created or edited using Gigapan software, Adobe Illustrator, and Adobe Photoshop.

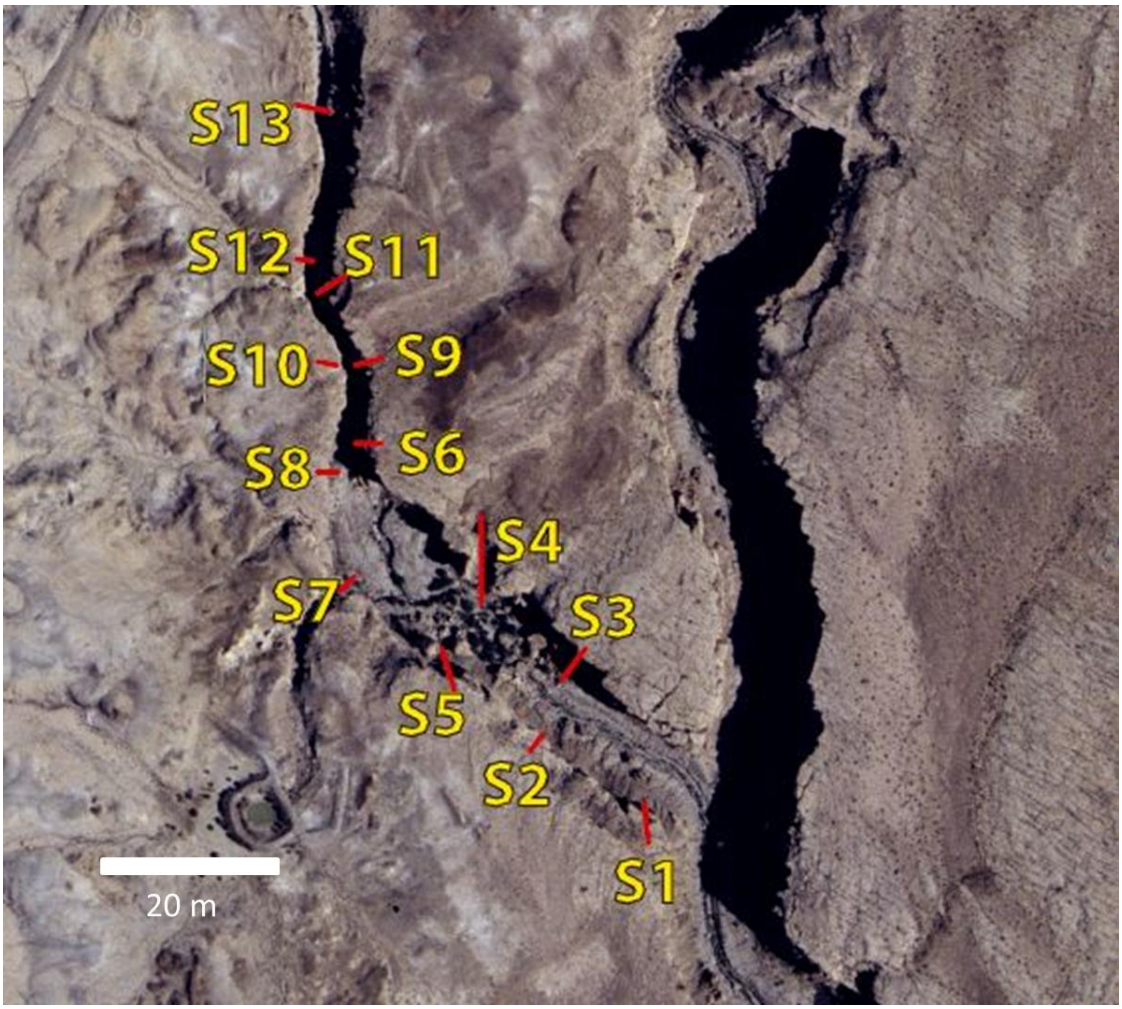

Figure 8. Aerial photograph taken of the western fork of Neilson Wash. Red lines indicate the location of the measured sections while yellow letters designate the name of the section.

In areas where the outcrop was inaccessible due to cliffs, measured sections were done using rappelling equipment. The incised valleys considered within this study cut into the marine deposits of parasequence 4 (Li et al., 2010) (fig. 6). Typical facies associations were used to determine the dominant formative process involved in the creation of a given channel story (Bhattacharya, 2006; Li et al., 2010; Zhu et al., 2012).

This was determined by evaluating the proportions of process-related facies associations within the IVS and using the most prolific process-related facies as the primary formative process. These facies associations include wave dominated shoreface associations and river dominated pro-delta to delta front associations (Bhattacharya, 2006; Li et al., 2010; Zhu et al., 2012). A detailed description of the facies encountered within the incised valley system can be found in table 2 along with an example measured section and legend in figure 9. Bounding surfaces found within the IVS were also ranked and ordered based on characteristics described by Miall, 1991 (Table 1).

Rank and Characteristics of Bounding Surfaces	Fluvial, Deltaic Depositional Units	Instantaneous Sedimentation Rate (m/ka)	Examples or Processes	Time Scale of Processes (a)
0 th-order, lamination surface	Lamina		Burst-sweep cycle	10^{-6}
1 st-order, set bounding surface	Ripple (microform)	10^{5}	Bedform migration	$10^{-5} - 10^{-4}$
1 st-order, set bounding surface	Diurnal dune increment, reactivation surface	10^{5}	Bedform migration	10^{-3}
2 nd-order, coset bounding surface	Dune (mesoform)	10^{4}	Bedform migration	$10^{-2} - 10^{-1}$
3 rd-order, slipping 5 - 20˚in direction of accretion.	Macroform growth increment	$10^{2} - 10^{3}$	Seasonal events, 10-year flood	$10^{0} - 10^{1}$
4 th-order, convex-up macroform top	Macroform, e.g., point bar, levee, splay	$10^{2} - 10^{3}$	100-year flood, bar migration	$10^{2} - 10^{3}$
5 th-order, flat to concave up channel base	Channel, Delta lobe	$10^{0} - 10^{1}$	Long term geomorphic process	$10^{3} - 10^{4}$
6 th-order, flat, regionally extensive	Channel belt sequence	10^{-1}	5th-order (Milankovitch) cycles	$10^{4} - 10^{5}$
7 th-order, sequence boundary; flat regionally extensive	Depositional system alluvial fan, sequence	$10^{-1} - 10^{-2}$	4th-order (Milankovitch) cycles	$10^{5} - 10^{6}$
8 th-order, regional disconformity	Basin-fill complex	$10^{-1} - 10^{-2}$	3rd-order cycles, Tectoncee and eustatic processes	$10^{6} - 10^{7}$

Table 1. Rank and characteristics of bounding surfaces. Modified from Miall, 1992.

In order to correlate the measured sections, the flooding surface on top of parasequence 5B was used as a stratigraphic basal datum for a variety of reasons. PS5B is a basal datum and, therefore, limits the distortion of stratigraphic relationships created by the use of upper datums (Bhattacharya, 2011) and (2) Li et al. (2012). Campbell (2013) and Hilton (2013) also used PS5B as their datum, which would reduce confusion when correlating this data to those studies (fig. 6). While this datum can be found and walked out throughout much of the study area, it is not always exposed in the northern portion of Neilson Wash. In areas where PS5B was not exposed, the top of PS5b had to be interpolated using the method of Hilton (in prep). In order to accomplish this, Hilton (2013) had to account for local structural trends in the area. This was done by mapping a regionally traceable bentonite horizon using a handheld Trimble Geoxt unit and antenna. Hilton (in prep) then constructed a structure map using 22 data points collected from the Trimble Geoxt. Then, using numerous EW and NS profiles in ESRI ArcMAP®, structural trends of 1.4˚ dip to the west and a 0.4˚ to the north were subtracted from raw LiDAR elevation data. Then, using corrected elevations, measured sections could be hung relative to the PS5B datum even in areas where this datum was not exposed. For a more in depth discussion on how this was done, reference Hilton, 2013.

Flood deposits within the incised valley system were recognized by a fining upward succession, which could be a result of waning floods. Often flood packages could be recognized by the presence of mud chips, which may be a product of reworking

of the floodplain or bar drapes during a flood event. The base of some flood deposits can be erosive in nature but this is not always a diagnostic feature. Channel and channel belts, on the other hand, were recognized because they often contain a highly erosive scour base along with a coarser-grained pebble and mud chip lag. The erosive base along with the scour deposits are indicative of a channel thalweg and in some cases can contain logs. Generally, channel deposits within the IVS contained multiple flood deposits. Due to the high amount of erosion and scour, it is possible that some of the flooding units were not identified. This is because the erosion from an overlying floodplain may have juxtaposed similar grain sizes against one another making them difficult to distinguish in outcrop.

Flow depths were also calculated based on the Leclair and Bridge (2001) method. This was done using the assumption that only one-third of the entire dune is preserved within the cross-set. Therefore, 335 total cross-set thicknesses were used to calculate the average dune height within Valley 3. The average dune height was then used to calculate average flow depth. Dune height scales to 6 – 10 times the flow depth. Cross-set thicknesses were also subdivided into their respective channel belts and flow depths were calculated for each individual channel belt within Valley 3. The mode of the data set or the range of the most frequently occurring cross-set thickness was also used to estimate flow depth. This was done based on the notion that the most commonly occurring cross-set thickness might be indicative of the dominant flow regime (Leclair and Bridge, 2001).

2.2 Facies Descriptions

Within the IVS, there were at least six different facies that were observed and recorded. The underlying marine strata can be divided into at least two separate and distinct facies. The following provides a description of each of these facies along with diagnostic features that where encountered within the facies. Table 2 provides a condensed overview of each of the facies and is frequently referred to within the body of the text.

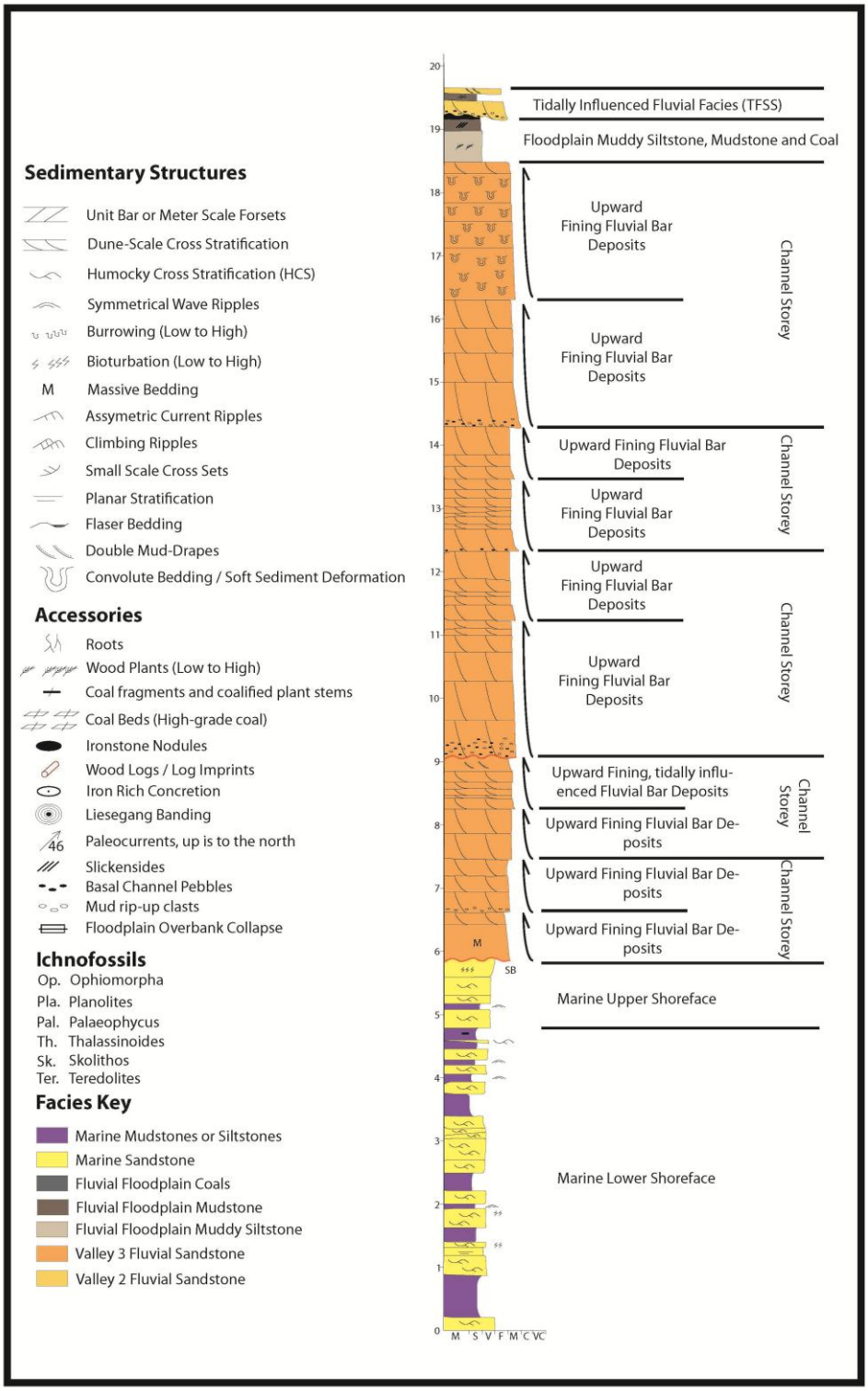

Figure 9. Example measured section S11 with corresponding legend and facies interpretation.

2.2.1 Marine Facies

Marine Upper Shoreface Facies (MU)

The marine upper shoreface facies is an upward-coarsening facies succession that consists of medium-upper to fine-upper grained sandstones. Diagnostic features of this facies include a high degree of burrowing from the *Skolithos, Ophiomorpha,* and *Glossifungities* ichnogenera. The bioturbation index (BI) for this facies ranges from 2 to as high as 6. Sedimentary structures include dune-scale trough stratification, hummocky and swaley cross stratification, planar bedding, and massive. Where present, this facies reaches a maximum thickness of 2 meters (fig. 9). However, throughout much of the study area it has been completely eroded by the overlying IVS.

Interpretation

The *Skolithos, Ophiomorpha,* and *Glossifungities* ichnogenera encountered within the MU is indicative of a shallow marine environment. These ichnofacies typically develop in marine environments in firm and unlithified substrates where relatively high levels of wave or current energy are typical (MacEachern et al., 2010). Hummocky and swaley cross stratification is also indicative of marine influence as it forms in response to the oscillatory motion induced by waves (Plint and Walker, 1992; Plint, 2010).

Marine Lower Shoreface Facies (ML)

The marine lower shoreface is composed predominantly of siltstones and mudstones interbedded with fine- to very fine-grained sandstones. Biota from this facies include fish scales and some plant material. Ichnogenera from the ML include *Ophiomorpha*, *Chondrites*, *Thalassinoidies*, and *Palaeophycus.* This facies can be found throughout the entirety of the study. Thickness can reach an excess of 15 meters but generally ranges from 3 – 6 meters in total thickness (fig. 9). The dominant sedimentary structure found within this facies is hummocky and swaley cross stratification but it also contains an abundance of ripple-scale cross stratification and planar cross stratification.

Interpretation

The ichnogenera found within this facies is also indicative of a marine environment. However, the heterolithic nature along with the finer grains found within the facies indicates that was a more distal environment than that of the MU. The abundance of hummocky and swaley cross stratification illustrates that this facies was below normal wave base but still above storm-wave base (Plint and Walker, 1992; Plint, 2010).

2.2.2 Facies of the Incised Valley System

Fluvial Sandstone Facies (FSS)

The most common facies encountered within the study area is that of the fluvial sandstone facies. This facies generally consists of coarse-lower to fine-grained sandstones that typically occur in fining upward successions and are bounded by concave-up scour surfaces. Often, this facies contains an erosive base with abundant extra-formational coarse-grained pebble lags and intraformational mudstone rip-up clasts (fig. 10). Locally, log jams and coal fragments can be observed at its base (fig. 10). Log jams typically contain an abundance of the *Teredolites* ichnofacies. Minor amounts of plant material and occasional mud drapes can also be found. This facies predominantly consists of dune- and ripple-scale cross stratification, but also contains varying degrees of planar beds, massive beds, and soft sediment deformation (fig. 10).

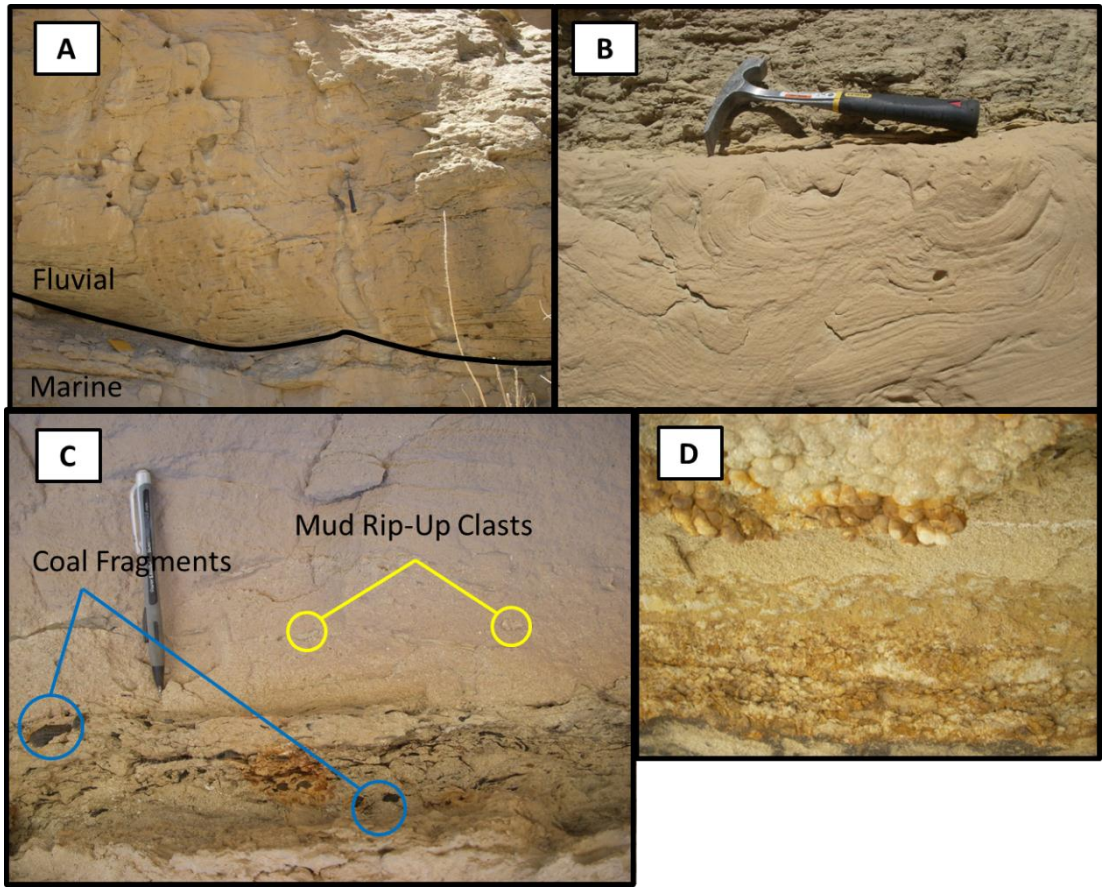

Figure 10A. The black line denotes the highly erosive scour base of the FSS facies into the upper shoreface facies. This line clearly denotes a change an increase in grain size as you move from the marine to the fluvial facies. The photograph also shows the dominant sedimentary structure, dune-scale cross stratification, within the fluvial facies. **10B** Illustration of soft sediment deformation that can be found within the FSS facies. **10C** Mud rip-up clasts and coal fragments that are associated with the erosive base of the FSS facies. **10D** Spherical nodules consisting of fine-grained sands intermingled with logs and other organic material. These nodules are diagnostic of small wood-boring crustaceans.

Interpretation

The FSS has been interpreted as classic fluvial deposits (Miall, 1996; Bridge, 2006; Miall, 2010). The erosive base found with the FSS has been interpreted to be the base of the channel. The mudstone rip-up clasts, pebble lags, and log jams that can be encountered within this facies is diagnostic of channel thalweg deposits. The mudstone rip-up clasts are probably intra-formational clasts that were entrained during the flood stages of the river and deposited as the flood wanes. The fining upward successions that can be found within the FSS are a result of waning floods or abandoned channel fills (fig. 9). Cross beds and other sedimentary structures within this facies represent active sites of deposition in the form of channel bars. Areas with soft sediment deformation indicate a very high rate of deposition and are probably a result of anomalously large floods. The presence of spherical nodules within this facies is diagnostic of wood-boring organisms which do provide evidence for some marine influence.

Tidally Influenced Fluvial Facies (TFSS)

Another important facies encountered within the study area is the tidally influenced fluvial facies. This facies is composed of medium- to very fine-grained sandstones that are interbedded with mudstones. This facies occurs in fining upward successions and often contains plant material including leaf impressions and *Planolites* burrows. Sedimentary structures consist of dune- and ripple-scale cross stratification, planar beds, climbing ripples, double mud drapes, mud-draped dune slip faces and soft-sediment deformation. In some cases, the dune-scale trough cross stratification displays bi-directional paleocurrent indicators (fig. 11).

Interpretation

Similar to the fluvial facies, cross beds and other sedimentary structures found within the TFSS represent active sites of deposition in the form of channel bars. However, the presence of double mud drapes, mud-draped dune slip faces, and bi-directional paleocurrents is likely a result of tidal reworking of sediments during spring and neap tides and indicate a subtidal depositional environment (Visser, 1980).

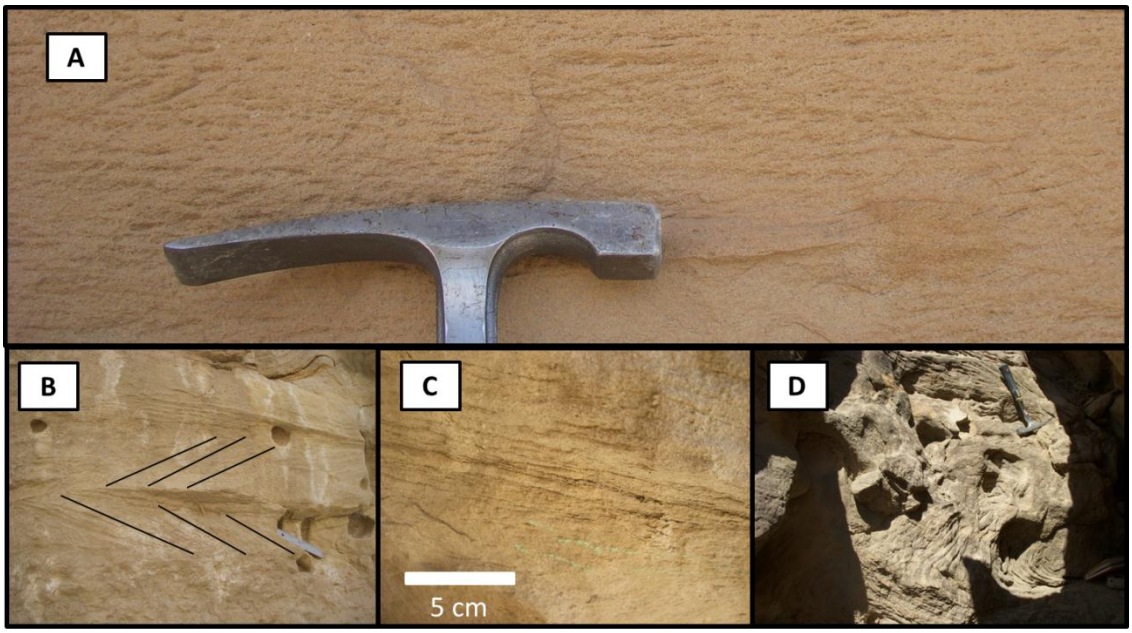

Figure 11A. Ripple-scale cross stratification associated with the TFSS facies. **11B** Dune-scale trough cross stratification displaying bi-directional paleocurrent indicators. **11C** Mud-draped dune slip faces. **11D** Soft-sediment deformation associated with the TFSS facies.

Abandoned Channel Facies (AC)

The abandoned channel facies is composed of very fine-grained sandstones, silt and mudstones. These deposits contain high amounts of organic material that include leaf imprints and root traces. In some instances, coal seams may also be found within this facies. Sparse trace fossil assemblages can be encountered within this facies that include *Planolites.* The dominant sedimentary structures within this facies include ripple-scale lamination and planar laminated silts and muds (fig. 12).

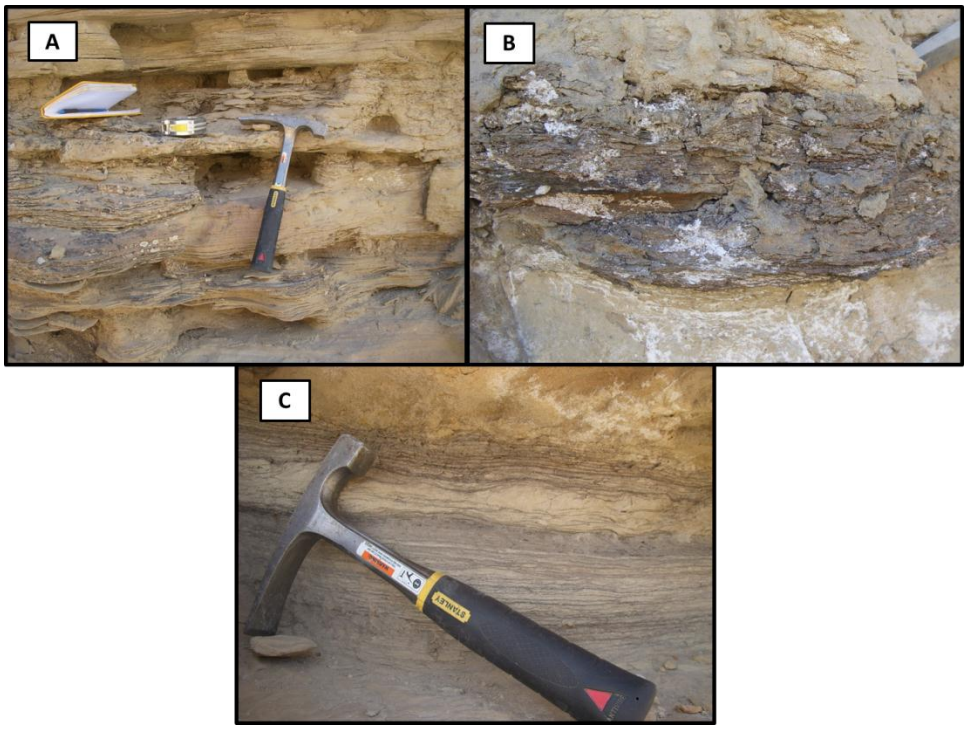

Figure 12A Planar laminated silts and muds along with some ripple-scale fine-grained sandstones associated with AC facies. **12B** Planar laminated mudstones. **12C** Ripple cross-laminated very fine-grained sandstones along with planar laminated silts and muds.

Interpretation

The very fine-grained sandstones, mudstones, and siltstones associated with this facies along with ripple- and planar-scale lamination is a result of a decrease in energy within the fluvial system that is most likely a product of river avulsion or river cutoff. The presence of root traces is also indicative of a low energy, low deposition environment that allows for the growth of plants.

Floodplain Facies (FP)

The floodplain facies typically occurs in fining upward successions that are characterized by mud and silt deposits that fine into pure mudstone. This facies contains abundant organic material that can include both leaf imprints and root traces. The FP facies may also contain rare ironstone siderite nodules. The facies contains abundant slickensides and is generally massive in nature. Although, ripple cross stratification, planar lamination, and flaser bedding can also be found (fig. 13).

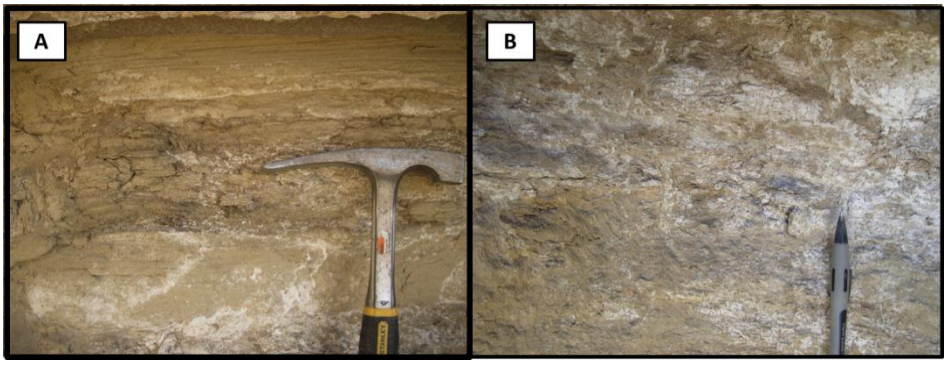

Figure 13A. Planar laminations located within the FP facies. **13B** Massive mud and silt deposits that are associated with the FP facies.

Interpretation

The presence of abundant organic material along with leaf imprints and root traces indicates a swamp like paleo-environment with anoxic conditions. Slickensides and root traces indicate that deposition was not continuous and that the area was exposed to multiple wet and dry cycles.

Estuarine Muddy Facies (EMF)

The estuarine muddy facies is primarily composed of mudstone and siltstone but may also contain some interbedded very fine grained sandstones. No apparent burrowing can be found within this facies but it does contain varying degrees of organic material and leaf impressions. The EMF facies can be massive in nature, but may also include planar lamination, ripple cross stratification, and some very low angle hummocky and swaley cross stratification.

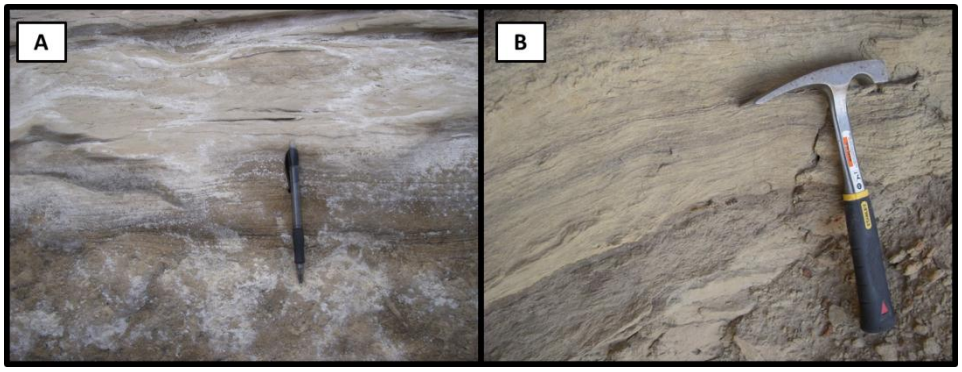

Figure 14A. Low-angle hummocky and swaley cross stratification located within the EMF. **14B** Ripple cross stratified siltstones within the EMF.

Interpretation

Planar laminations and ripple laminations along with the lack of root traces and slickensides indicate a relatively continuous rate of deposition with none of the wetting and drying cycles that are associated with the FP. The presence of hummocky and swaley cross stratification is also indicative of marine influence and is probably a result of large storms reworking the sediments (Plint and Walker, 1992).

Facies	Lithology	Biota	Sedimentary Structures
Fluvial Sandstone (FSS)	Very-fine to coarse-lower grained sandstones. Typically fining upward successions that contain pebble lags, mudstone rip-up clasts and ocassional mud drapes.	Logs, plant material, very minor amounts of coal, T*eredolites* is common in logs.	Predominantly dune and ripple scale trough cross stratification, planner beds, massive beds, soft sediment deformation, mud rip-up clasts.
Tidally Influenced Fluvial (TFSS)	Medium to very fine grained sandstones interbedded with mudstones, fining upward.	Leaf impressions, some plant material, *Planolites* burrows.	Dune and ripple scale trough cross stratification (some displaying bi-directional paleocurrent indicators), planar cross stratification, climbing ripples, double mud drapes, mud draped dune slipfaces, soft sediment deformation.
Large Scale Inclined Strata (LSIS)	Medium-upper to fine-upper grained sandstone, Generally upward fining beds.	No plant material and no apparent burrowing.	Cross beds (avalanch faces) draped with dune scale trough cross stratified bed forms.
Abandoned Channel (AC)	Very fine grained sandstones, silt and mudstones.	High amounts of plant material and abundant leaf impressions. Contians coal seams. Sparse trace fossil assemblages including O*phiomorpha* and *Planolites.*	Ripple scale cross lamination and, planer laminated silts and muds.
Floodplain (FP)	Typically occur in fining upward successions. Dominantly mud and silt deposits that fine into pure mudstone.	Abundant organic material, leaf imprints, root traces. Contains Ironstone Siderite Nodules.	Massive, ripple cross stratification (splays), planar lamination and flaser bedding. Contain numerous slickenslides.
Inclined Heterolithics (IH)	Very fine to fine grained sandstones with abundant silt and mud drapes.	Plant material and leaf impressions. Skolithos, Planolites and Beaconites burrows.	Dune scale trough cross stratification, Ripple scale cross stratification, climbing ripples, double mud drapes, lenticular bedding and soft sediment deformation.
Estuarine Muddy Facies (EMF)	Primarily mudstones and siltstone. Contains some interbedded very find grained sandstones.	Leaf impressions, plant material, no apparent burrows.	Massive, planar lamination, ripple cross stratification, hummocky and swaley cross stratification, siderite nodules.
Marine Upper Shoreface (MU)	Medium-upper to fine-upper grained sandstones.	High degree of burrowing near the top. Some carbonaceous material. Icnogenera include: *Skolithos*, *Ophiomorpha* and *Glossifungitis*.	Dune scale trough stratification, hummocky and swaley cross stratification, planar bedding and massive.
Marine Lower Shoreface (ML)	Siltstones interbedded with very fine grained to fine grained sandstones.	Fish scales, some plant material, *Ophiomorpha*, *Chrondrites*, *Thalassinoidies*, *Palaeophycus*.	Hummocky and swaley cross stratification, ripple scale cross stratification, planer cross stratification, massive.

Table 2. Facies descriptions

SECTION 3. VALLEY FILL AND ARCHITECTURE

3.1 Overview

Data collected from outcrop within Neilson Wash indicates the presence of a complex incised valley fill. The three incised valley systems within the region include: Valley 1 (youngest in age), Valley 2, and Valley 3 (oldest in age). However, within the study area, only Valley 3 and portions of Valley 2 can be found. Incised valleys were identified by; (1) an abrupt basinward shift in depositional facies across a sharp erosional contact (2) stratal truncation and onlap of fluvial units on top of marine and (3) valley heights that are several times higher than that of a single channel fill (fig. 15). There is also evidence for fluvial terraces within Valley 3, as it contains at least four cut and fill episodes. Valley fill within the two valleys is dominantly fluvial, with a smaller degree of tidal and floodplain deposits respectively. These separate cut and fill episodes were identified by: (1) regionally traceable erosional surfaces, (2) truncation and onlap of beds, (3) differences between facies and biota encountered above and below erosional surfaces, (4) incision that is greater than that of a single channel storey, and (5) differences in paleo-hydraulics (Campbell, 2013).

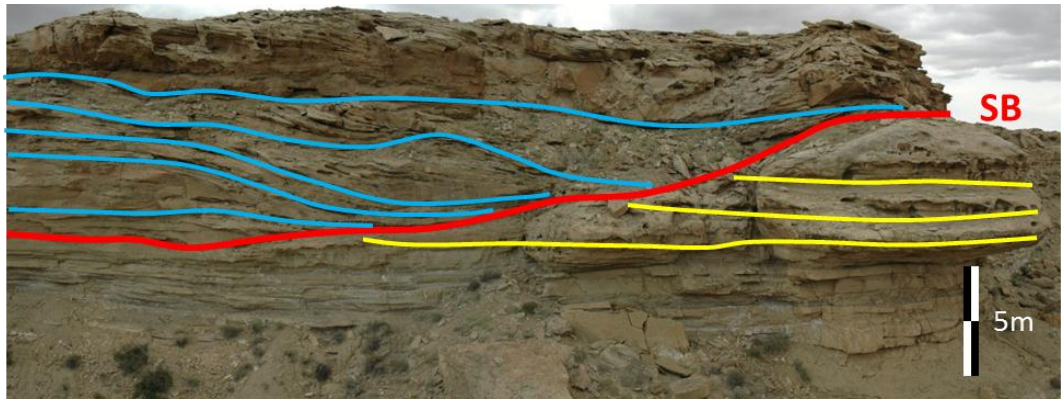

Figure 15. Gigapan image taken of the study area demonstrating the criteria for the recognition of an incised valley. Blue lines represent fluvial strata, the red line represents the sequence boundary (SB) and the yellow lines indicate marine units.

3.2 Valley 3

Valley 3 shows a minimum of five cut and fill episodes that are associated with different channel belts. The V3 system contains fill from at least 2 valley systems termed Valley 3A and Valley 3B (fig. 16 & 17). V3 formed as a result of multiple sea-level fluctuations and incised into the lower shoreface deposits of parasequence 4 (fig. 6). Relative ages for the two incised valleys were determined based on cross-cutting relationships observed in outcrop (fig. 16 & 17).

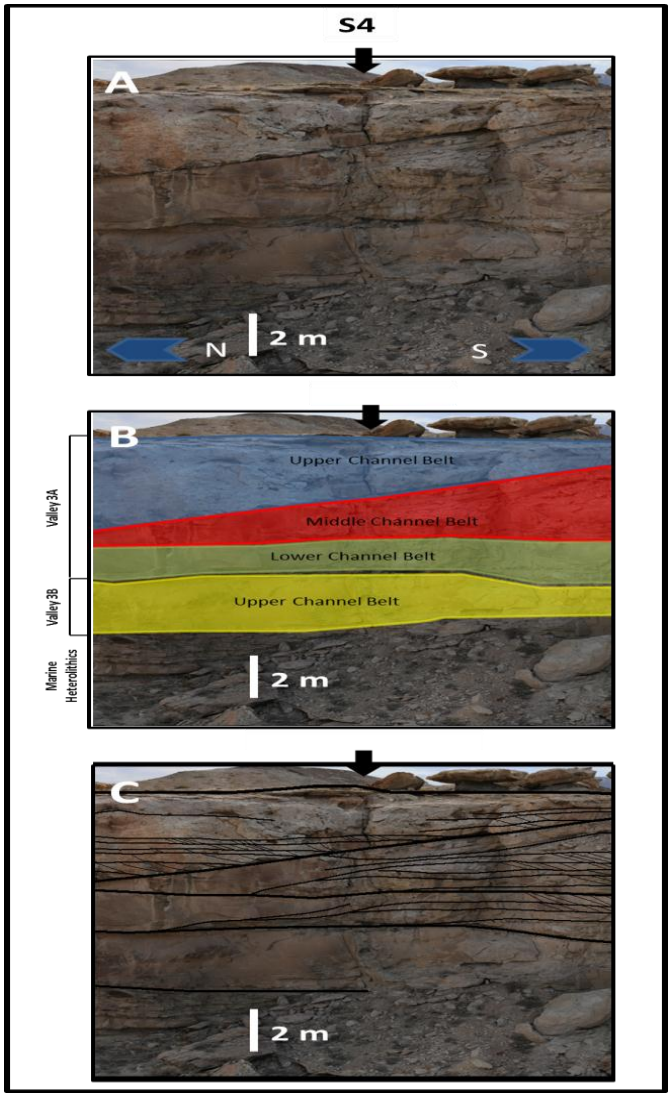

Figure 16. Bedding architecture and facies of Valley 3. This was taken facing east and is a portion of the eastern cliff face of Neilson Wash. A) Photomosaic of the eastern cliff face of Neilson Wash. Measured section S4 was taken along the northern portion of the photomosaic. B) Valley 3 can be subdivided into Valley 3A and Valley 3B. This complex incised valley systems formed in response to multiple cut and fill episode as evidenced by the presence of at least 4 channel belts within the incised valley system. C) Internal organization and bedding architecture of the incised valley system.

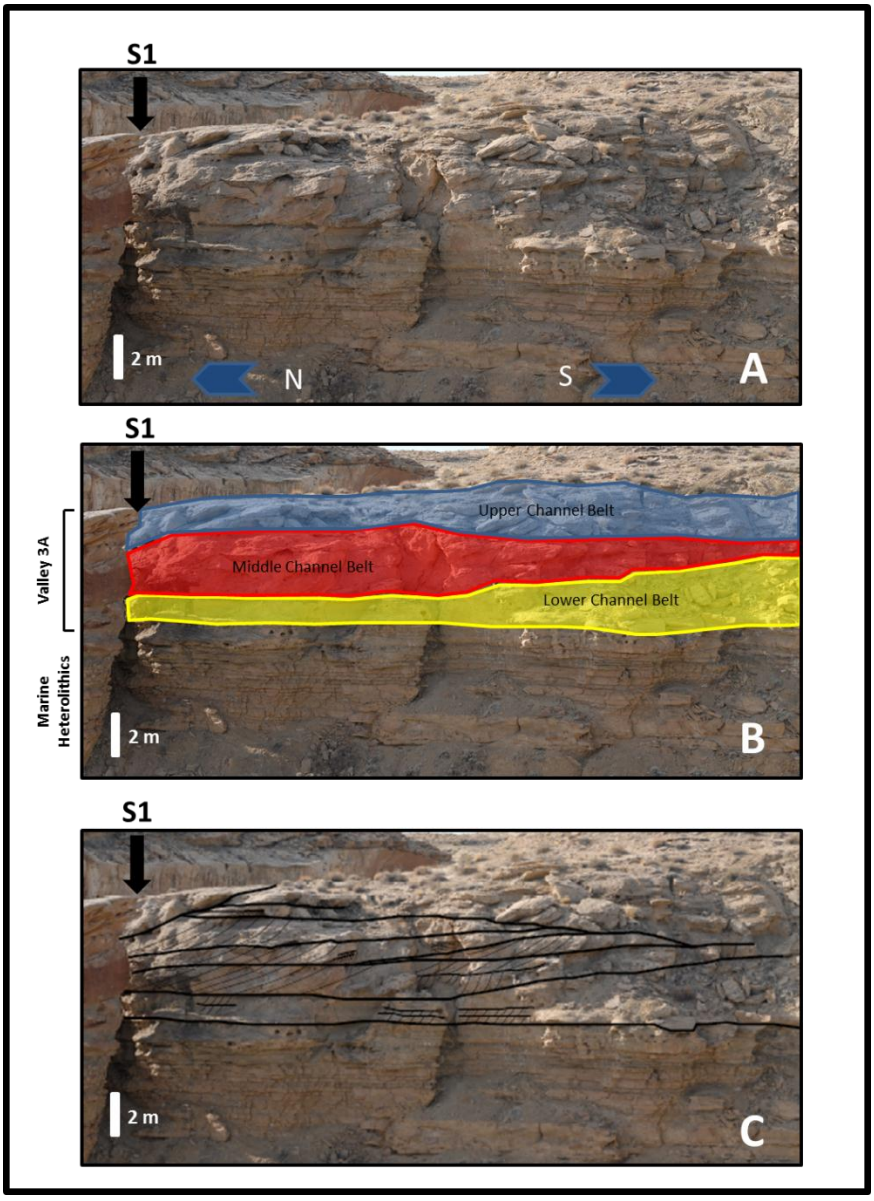

Figure 17. Bedding architecture and facies of Valley 3. This was taken facing east and is a portion of the eastern cliff face of Neilson Wash. A) A portion of the eastern cliff face of Neilson Wash. Measured section S1 was taken along the northern portion of the photomosaic. B) Valley 3B is not present in this portion of the study area. However, Valley 3A can be subdivided into three separate channel belts. C) Internal organization and bedding architecture of the incised valley system.

3.2.1 Valley 3B

The oldest deposits located in the study area are those of Valley 3B (V3B), which can be found in the northern portion of the study area (fig. 18 & fig. 19). Less than approximately 4 m of outcrop exposure exist for V3B within the study area. V3B deposits were recognized because they contain non-marine fluvial strata that have incised into the lower shoreface deposits of parasequence 4. The composite sequence boundary that is located at the base of V3B is an 8th order surface (*sensu* Miall, 2002) that can be traced regionally and is found immediately beneath all of the valley fill within the study area.

The Lower Channel Belt – V3B

Two very distinct channel belts are exposed within V3B. Unfortunately, due to lack of exposure, a maximum of 1 m of the lower channel belt is exposed. The limited outcrop of the lower channel belt consists primarily of massive, highly weathered sandstone and is found only in the northern portion of the study area in S9 – S13 (Fig. 18 & 19). It is generally massive but was found to contain some trough cross-stratified sandstones with sets ranging from about 10 cm up to nearly 40 cm. Grain sizes within this channel belt ranged from medium upper to medium lower. This lower channel belt is capped by an erosive 6th order surface. Due to the lack of exposure, only 11 paleocurrent measurements and 5 bar accretion measurements were obtained for this channel belt. Paleocurrent measurements were northwest while bar accretion deposits showed a south- southeast direction (fig. 20).

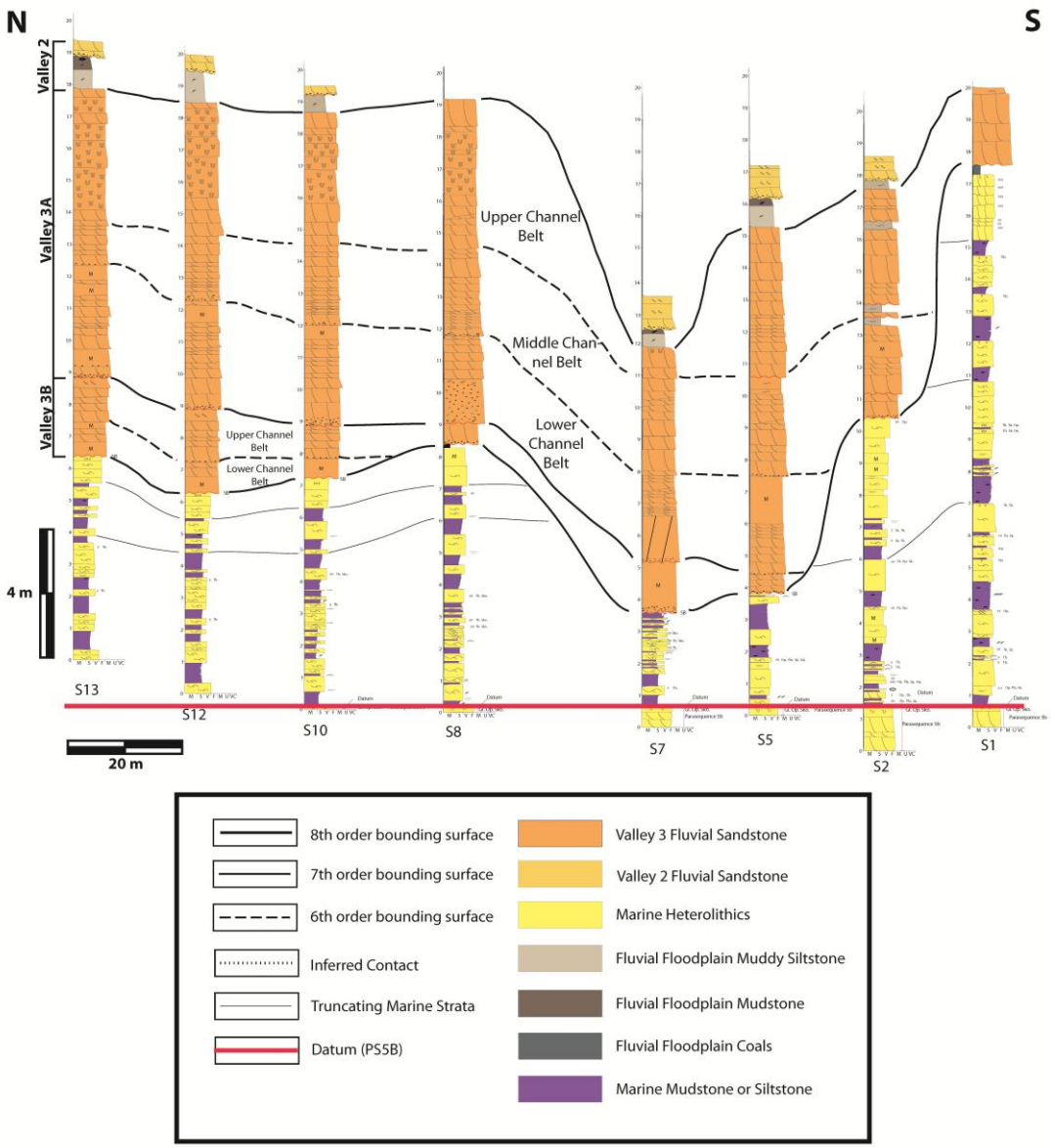

Figure 18. Measured sections taken along the western cliff face of Neilson Wash. Figure shows the geometry of Valley 3 which can be subdivided into Valley 3A and Valley 3B with their respective channel belts.

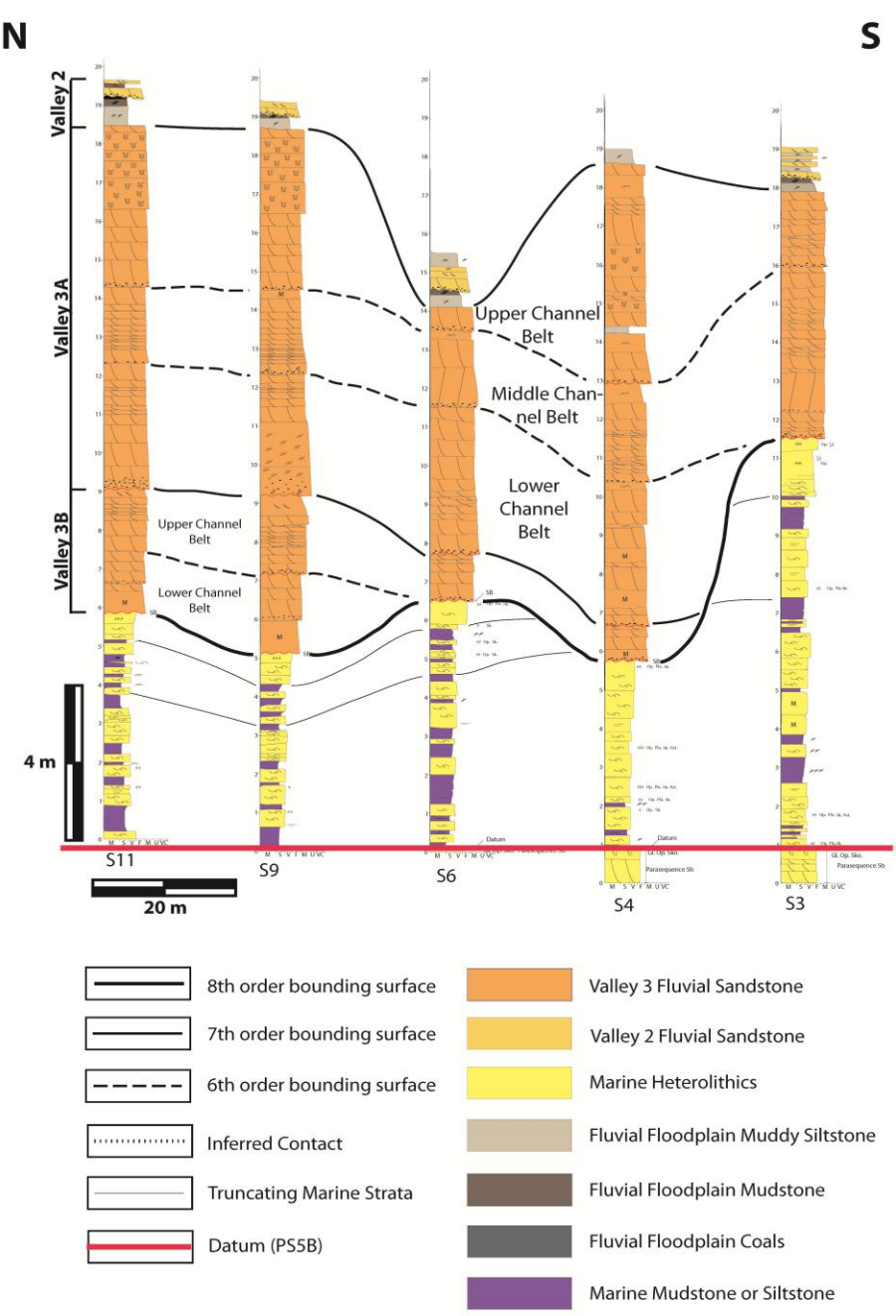

Figure 19. Measured sections taken along the eastern cliff face of Neilson Wash. Correlations show 6th, 7th and 8th order surfaces encountered within Neilson Wash. Figure also demonstrates the internal geometry of Valley 3 along with its constituent components.

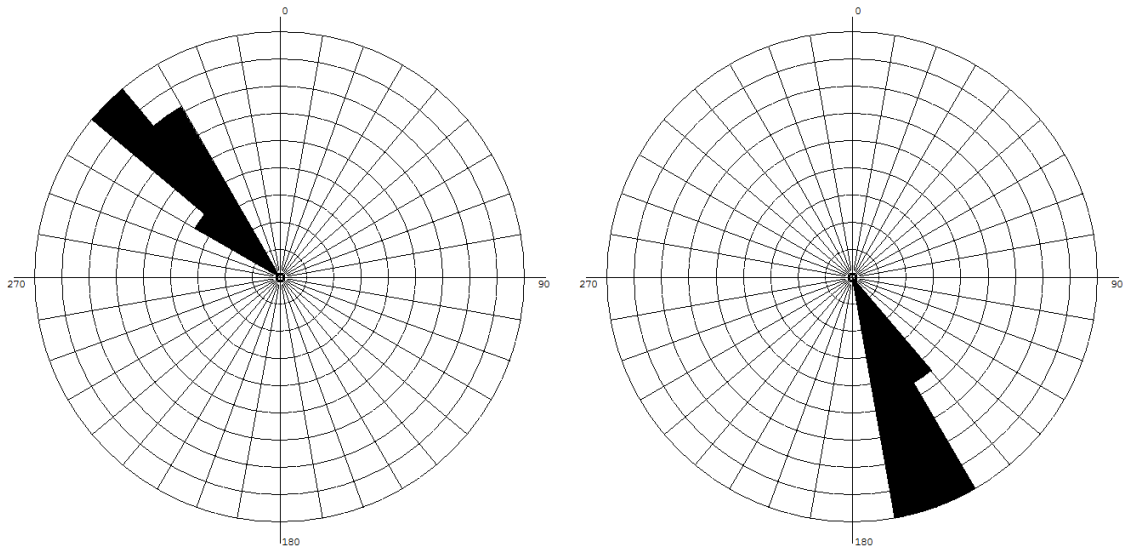

Paleocurrent Direction

N = 11

Bar Accretion

N = 5

Figure 20. Paleocurrent and bar accretion directions for the lower channel belt within Valley 3B.

The Upper Channel Belt – V3B

The upper channel belt is composed predominantly of trough cross-stratified sandstones but also contains ripple cross-stratified sandstones with some massive sandstones near its base. This channel belt can be found throughout nearly the entire study area and can reach thicknesses of approximately 2.5 m. Grain sizes for the upper channel belt range from medium-upper to medium-lower in the trough cross stratified sands and fine-upper to very fine-lower in the ripple cross-stratified sands. In some instances, both single and double mud drapes cap the rippled sandstones and muddy

lamina within the dune sets can also be found. Paleocurrent measurements and bar accretion deposits from this belt show a northeast direction (fig. 21).

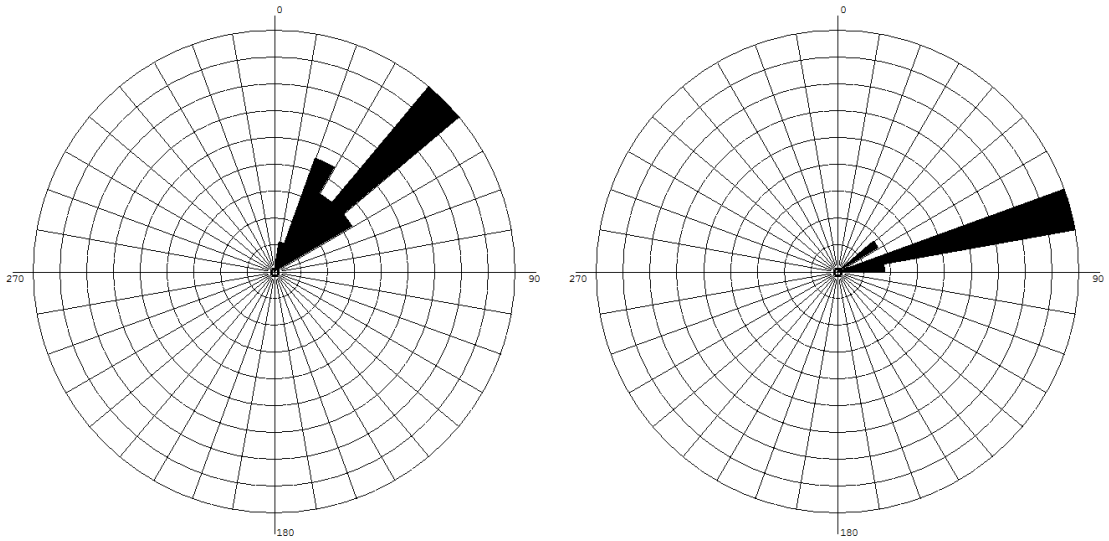

Figure 21. Paleocurrent and bar accretion directions for the upper channel belt within Valley 3B.

Interpretation

Due to the lack of outcrop exposure, it is difficult to determine the style and size of the channel belts located with V3B. The lower channel belt is composed entirely of fluvial FSS facies with no evidence of tidal or marine influence (table 1). Only 1st order surfaces can be found within the 3D trough cross-stratified sandstones of the lower channel belt. This lack of higher order surfaces indicates that only a single flood event is

exposed above the modern valley floor. Bar accretion directions and paleocurrent measurements taken from the lower channel belt occur in nearly opposite directions which is indicative of upstream accretion. The upper channel belt, however, has been interpreted as the tidally influenced fluvial facies (TFSS) which is indicated by the tidal couplets and muddy lamina found within the ripple cross-stratified and trough cross-stratified sands (table 2). The upper channel belt seems to have formed in response to at least two major flooding events that have stacked to form a compound bar and are separated by 3rd order boundaries. These flood deposits are fining upward in nature and generally grade from medium grained trough cross stratified sands to very fine lower ripple cross-stratified sands. Thickness of these flood packages range from 20 cm to 1 m. Paleocurrents measured from this outcrop are generally north to northeast and form roughly parallel to the dip of surfaces within the compound bar suggesting that bar formation had a component of downstream accretion (fig. 21).

3.2.2 Valley 3A

Fill from Valley 3A (V3A) can be found throughout the entirety of the study area. Its thickness ranges from 3 meters up to 13 meters and in certain localities, it erodes to within 3 meters of the datum (parasequence 4). Criteria that were used to identify this valley included: 1) truncation and erosion of either Valley 3B or marine deposits and 2) deposits are thicker than a single channel story. Valley 3A is bounded above by a 7th order surface and below by a 7th order surface where it erodes into Valley 3B. This 7th order surface changes to an 8th order surface where the valley erodes into marine units.

Valley 3A contains an overall fining upward succession and contains a pebble lag, rip-up clasts, logs, and mud chip conglomerates throughout much of its base (fig. 22). Paleocurrents taken from Valley 3A give a general northeastern trend.

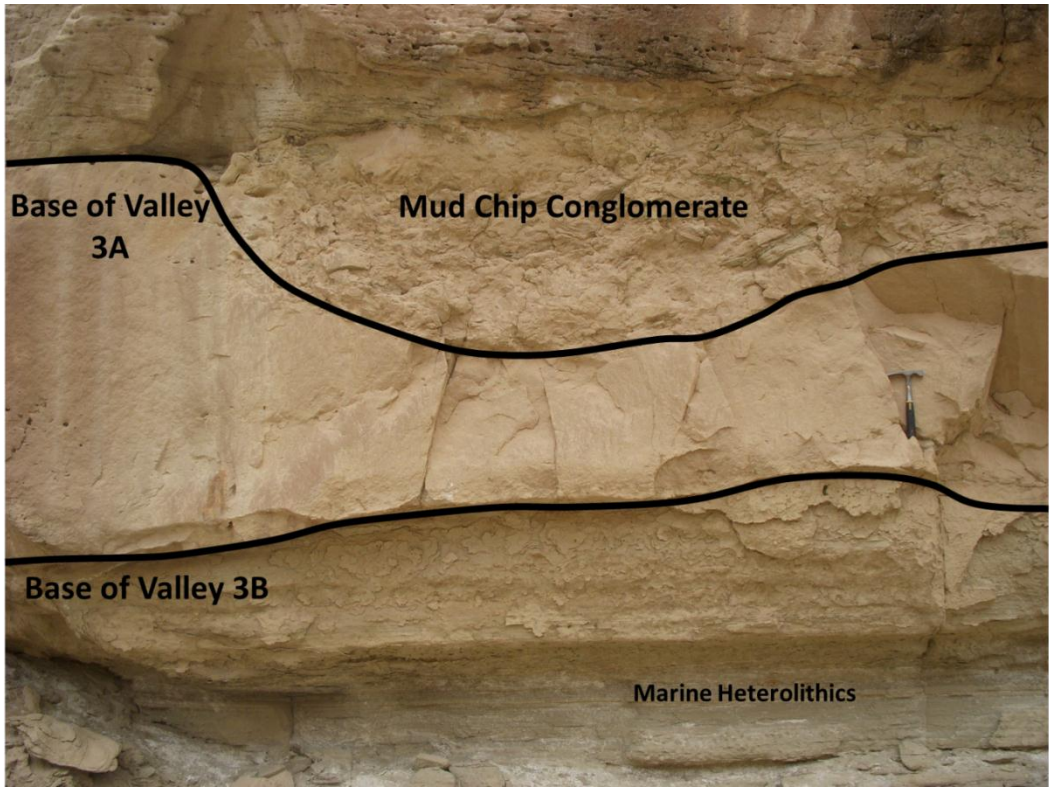

Figure 22. A mud chip conglomerate associated with a basal scour of the lower most channel belt of Valley 3A.

The Lower Channel Belt – V3A

The basal channel belt located within Valley 3A can be found along nearly the entire length of valley. It is bounded below by either a 7^{th} or 8^{th} order bounding surface (as described above) and above by a 6^{th} order surface that separates it from a younger channel belt (fig. 18 & 19). The channel belt reaches nearly 3.5 meters in total thickness

near the maximum incision point. This channel belt is composed of predominantly fluvial facies (FSS) (table 1) with grain sizes that range from coarse-lower to fine-upper. Preserved cross-set thicknesses range from 5 cm to approximately 60 cm in total thickness. In general, cross-set thicknesses decrease as you move from the base of the channel belt to the top. Multiple 3rd order surfaces can also be found within this channel belt representing individual flood packages. These packages range in thickness from half a meter to 2 meters. Each individual flood unit is a fining upward succession and generally ranges from medium-upper to fine-upper in grain size. Paleocurrent measurements taken from this channel belt give a northeasterly trend while bar accretion is expanding to the east (fig. 23).

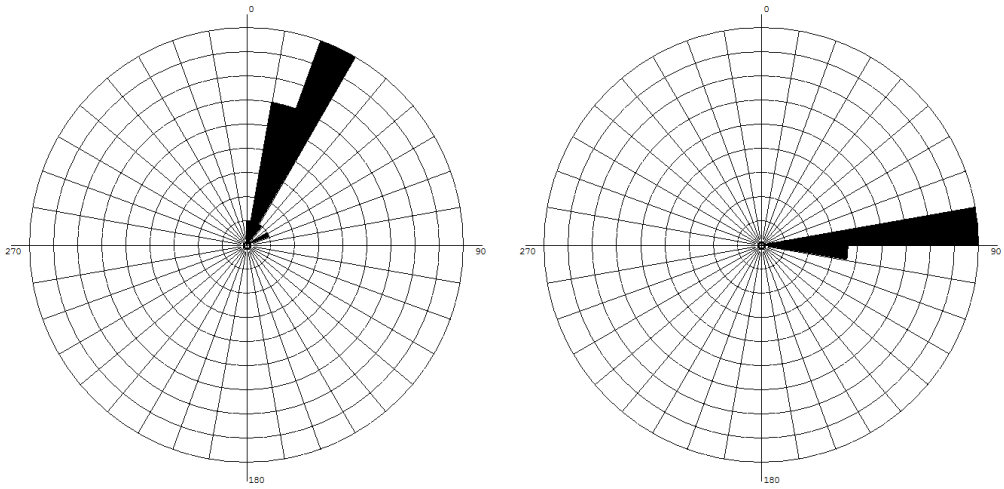

Paleocurrent Direction **Bar Accretion**

N = 18 N = 7

Figure 23. Paleocurrent and bar accretions directions for the lower channel belt located within Valley 3A.

The Middle Channel Belt – V3A

The middle channel belt associated with Valley 3B runs along the entire extent of the incised valley system and is composed entirely of the FSS fluvial facies (table 2). At its base, the channel belt is bounded by a 6^{th} order bounding surface, which can be recognized by a sharp erosional contact that contains mud chips and organic material. The channel belt is bounded above and below by a 6^{th} order surface that separates it from the lower and upper channel belts respectively. The middle channel belt is composed predominantly of trough cross-stratified sands and contains very little ripple cross-stratification. Grain sizes within this unit range from medium-upper to fine-upper but are dominantly medium to medium-lower sands. Like the lower channel belt, this channel contains numerous 3^{rd} order bounding surfaces indicating individual flood deposits. The thickest flood deposits can be found at the base of the channel and range in thickness from 1 m to 20 cm. At its thickest point, the channel belt reaches approximately 4.5 meters. Cross-set thicknesses within these flood deposits also range in thickness from 5 cm to 1 m with the larger cross-sets typically occurring within the larger flood units. Paleocurrent measurements taken from the northern end of the channel belt show a northwesterly direction which, moving south, changes to a more northeasterly direction. However, bedding within this channel remains fairly consistent and dips eastward (fig. 24).

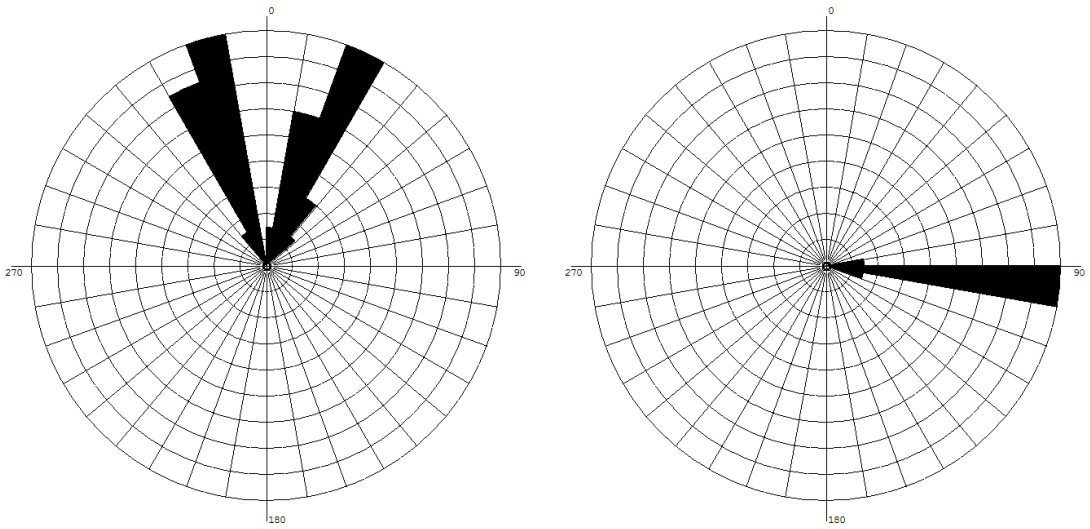

Figure 24. Paleocurrent and bar accretion directions for the middle channel belt within Valley 3A.

The Upper Channel Belt – V3A

Similarly, the upper channel belt is located throughout the entire study area. At its base there is a sharp erosional 6th order surface that is characterized by a mud chip lag (fig. 25). The uppermost channel belt reaches nearly 5 meters in thickness and is bounded above by an 8th order surface that separates it from Valley 2. This channel belt is also composed of the fluvial (FSS) facies and contains trough cross-stratified sandstones. However, this channel belt is unique as it contains a high degree of soft-sediment deformation. Unlike the other channel belts within V3B, this channel contains well preserved ripple cross stratification due to the lower degree of erosion from the

overlying Valley 2 deposits. Similar to the other channel belts, flood deposits found within the upper channel belt are thicker near the bottom of the channel and thin moving upward (fig. 25). 3rd order surfaces are contained within the channel belt that give paleocurrent measurements in an east- northeast direction. Bar accretion directions for this channel give a west- southwest direction (fig. 26).

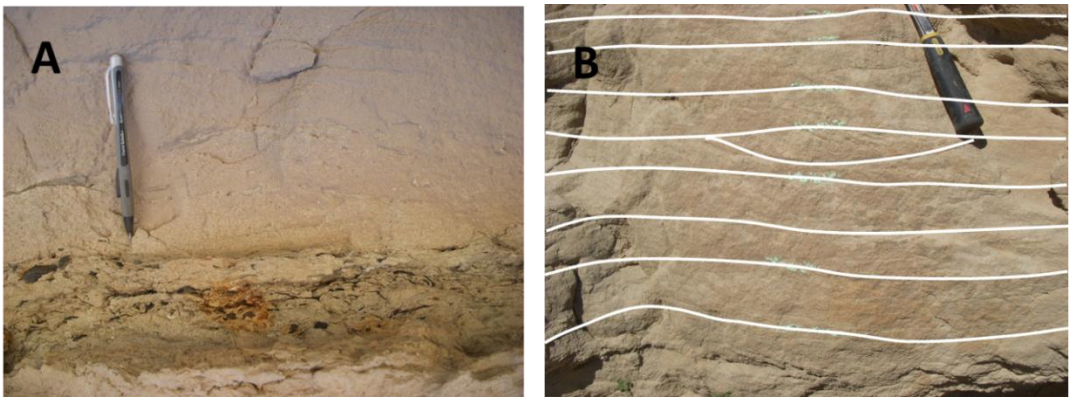

Figure 25. A) Mud chip lag that can be found at the base of the upper channel belt within Valley 3A B) 3D dune sets within the upper channel belt get progressively thinner toward the top of the channel. White surfaces indicate 1st order bounding surfaces.

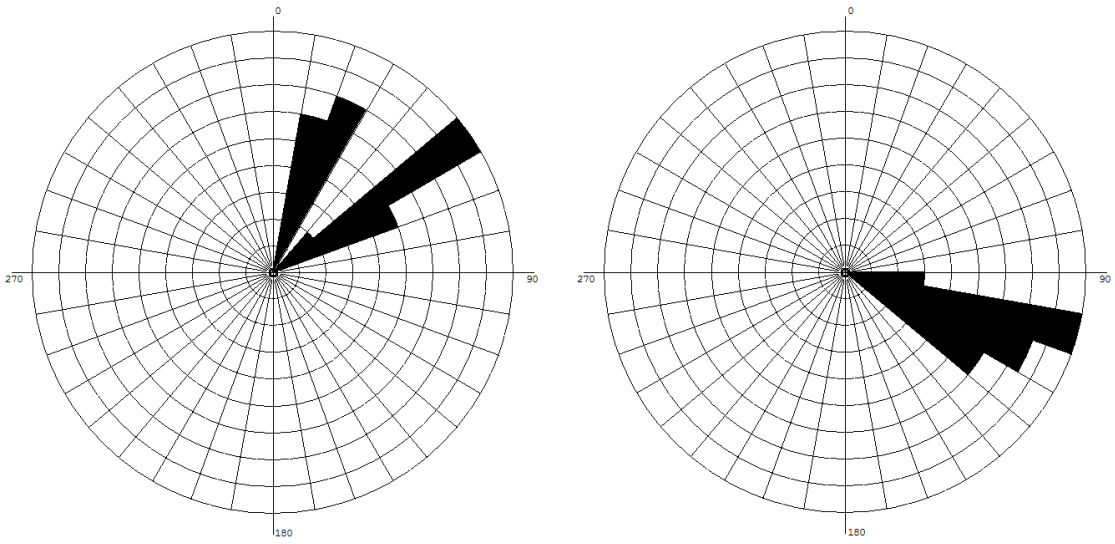

Figure 26. Paleocurrent and bar accretion directions for the upper channel belt within Valley 3A

Interpretation

Valley 3A is composed primarily of laterally accreting points bars as the paleocurrents measured within V3A occur at oblique angles to the internal bedding surfaces (fig. 23, 24 & 26). The presence of multiple 3rd order bounding surfaces within the channel belts of V3A indicate that they formed in response to multiple flooding events. Flood packages within V3A range from approximately 20 centimeters to 1.5 meters. These flood deposits are fining upward in nature and generally grade from medium-grained trough cross-stratified sands to very fine lower ripple cross-stratified

sands. The presence of highly preserved ripple cross stratified sandstones within the upper channel belt are probably indicative of the fluvial system changing from highly amalgamated, transgressive deposits to that of the muddier, unconfined highstand deposits of Valley 2. The lack of a tidal signature within these deposits indicates that V3A is composed entirely of the fluvial FSS facies (table 2).

3.3 Valley 2

Only a portion of Valley 2 can be found within the study area (fig. 18 & 19). This portion of the study area has been interpreted to be Valley 2A. Criteria used for the identification of this valley system include: (1) valley incision into Valley 3, (2) deposits onlap and downlap onto the valley margin and the deposits truncate underlying Valley 3 deposits, and (3) the depth of incision was greater than that of a single channel form. Like Valley 3, Valley 2 can be broken down into Valley 2B and Valley 2A deposits, which can be further subdivided into different channel belts. However, only the lowermost channel belt within Valley 2A and Valley 2B are encountered within the study area. Overall, grain sizes found within this valley are considerably finer grained than that of Valley 3.

3.3.1 Valley 2A

Valley 2A can be found throughout the entire northern half of the study area and reaches as far south as S9. However, Valley 2A contains much more heterolithics that are composed of the tidally influenced fluvial facies (TFSS), floodplain deposits (FS), and

in some cases abandoned channel deposits (AC) (Table 1). The sequence boundary at the base of this incised valley system has been termed Sequence Boundary 1 by Li et al, (2010) and Zhu (2010) and is an 8th order boundary. The erosional surface found at the base of this valley is characterized by coarser grained pebble lag and a high degree of organic material. Only approximately 1.5 m of the lowermost channel belt are preserved within the study area. Overall, grain sizes found within this valley are considerably finer grained than that of Valley 3.

3.4 Paleo-hydraulics

Due to the high degree of incision within these amalgamated sands, it is difficult to determine the depth of channels. However, in order to estimate flow depth, 335 cross-set thickness were measured within Valley 3 and plotted in figures 27 and 28. These figures show the frequency of occurrence of preserved cross-set thickness measurements. Maximum flow depths can be assumed to approximate channel depths, while minimum flow depths probably represents low stage flow within the channel. The average cross-set thickness value for the whole of Valley 3 was determined to be 18.1 centimeters which, in turn, gives an average dune height of 54.2 centimeters. Dune heights are calculated to be three times that of the preserved cross-set thickness. Paleo-flow depth measurements were then estimated using the average dune height and were found to be between 3.3 and 5.4 meters (Leclair and Bridge, 2001). The second graph (fig. 26) uses the same data but has been modified to show the range of the most frequently occurring measurements (D'Souza, 2013). This was done to

estimate the dominant flow regime found within Valley 3 (Leclair and Bridge, 2011). This graph shows that the most frequently occurring cross-set thickness values occurred between 7 to 12 centimeters. These values would give an average dune height of between 20 to 38 centimeters and an average paleo-flow depth of 1.2 to 3.8 meters.

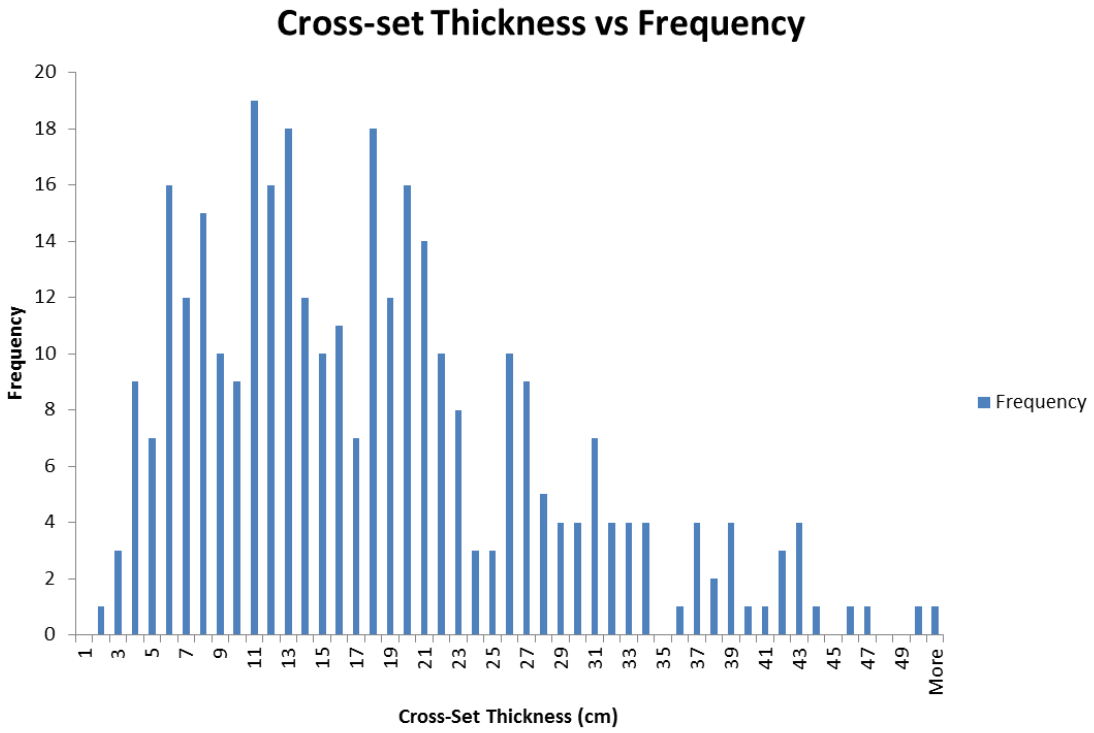

Figure 27. Graph showing cross-set thickness values versus frequency in which they occur for all channel belts within Valley 3.

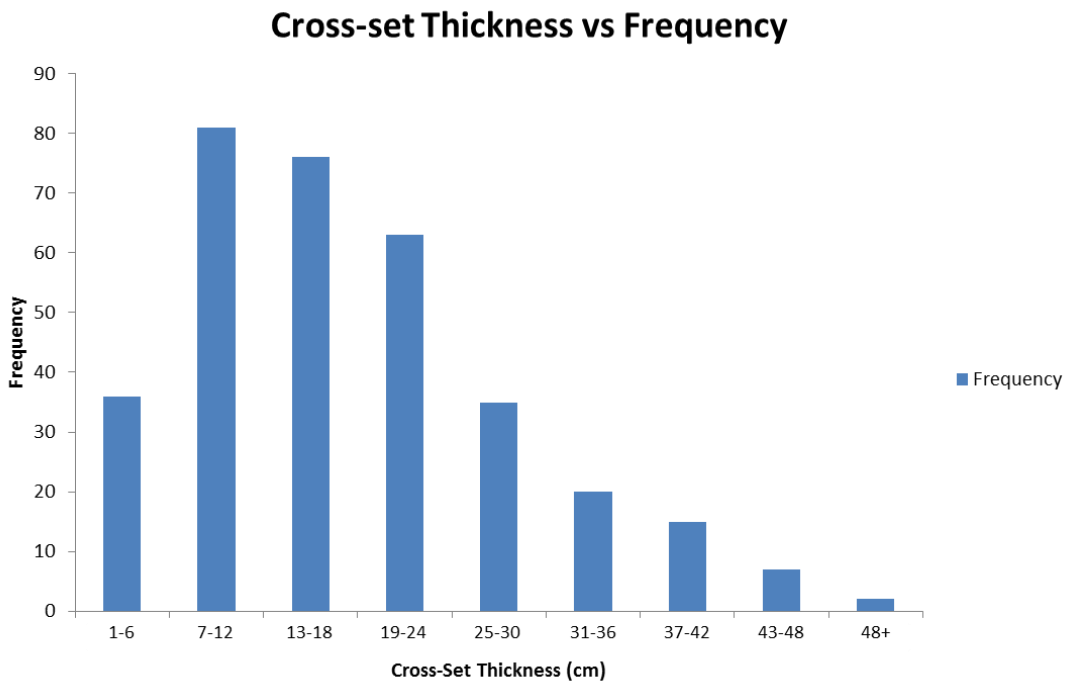

Figure 28. Graph showing cross-set thickness values versus frequency in which they occur for all channel belts within Valley 3. This graph has been modified to show the range of the most frequently occurring cross-set thicknesses.

3.4.1 Paleo-hydraulics of Valley 3B

Similarly, these 335 cross-set thicknesses were assigned to their appropriate channel belt and paleo-channel depths were estimated. Due to the lack of exposure for the lower channel belt within Valley 3B, an insufficient amount of cross-set thicknesses were obtained to accurately constrain paleo-channel depths.

Upper Channel Belt – Valley 3B

A total of 48 cross-set thicknesses were measured within the upper channel belt of Valley 3b (fig. 29). The average thickness for the cross-sets within this belt is 19.8

centimeters, thus giving a dune height of 59.5 centimeters and paleo-flow depths of between 3.6 and 6.0 meters (Leclair and Bridge, 2001). The cross-set thickness values that occur most frequently within this channel belt occur between 19 and 24 centimeters (fig. 30). This gives average dune heights of between 57 and 72 centimeters and flow depths of 3.4 to 7.2 meters.

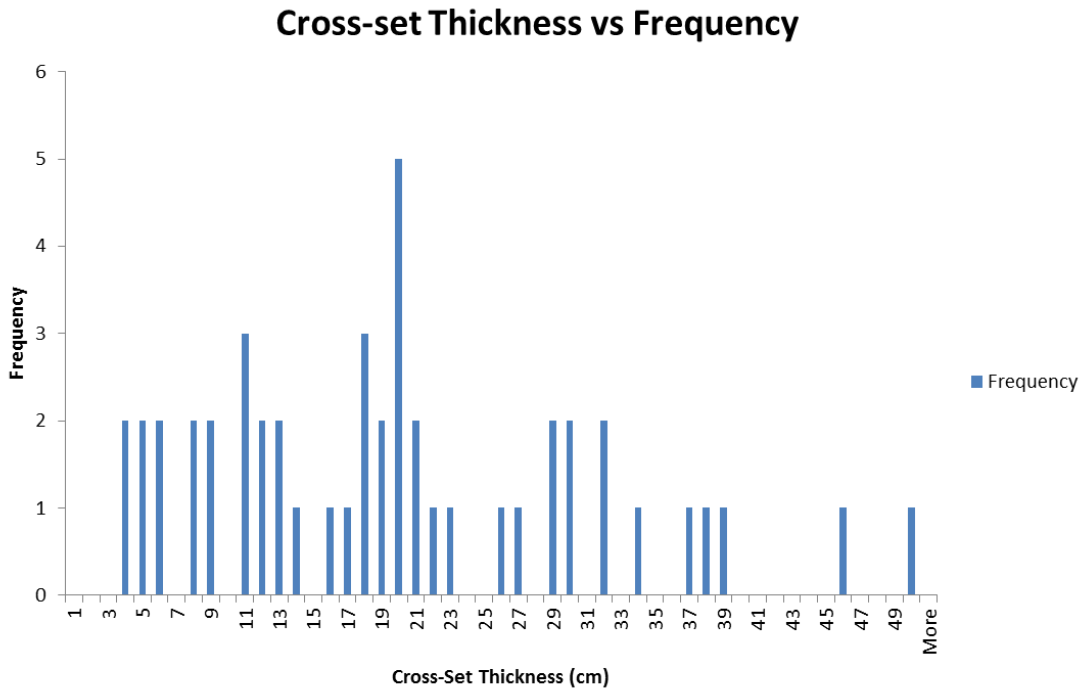

Figure 29. Graph showing cross-set thickness values versus frequency in which they occur for measurements taken within the upper channel belt of Valley 3B.

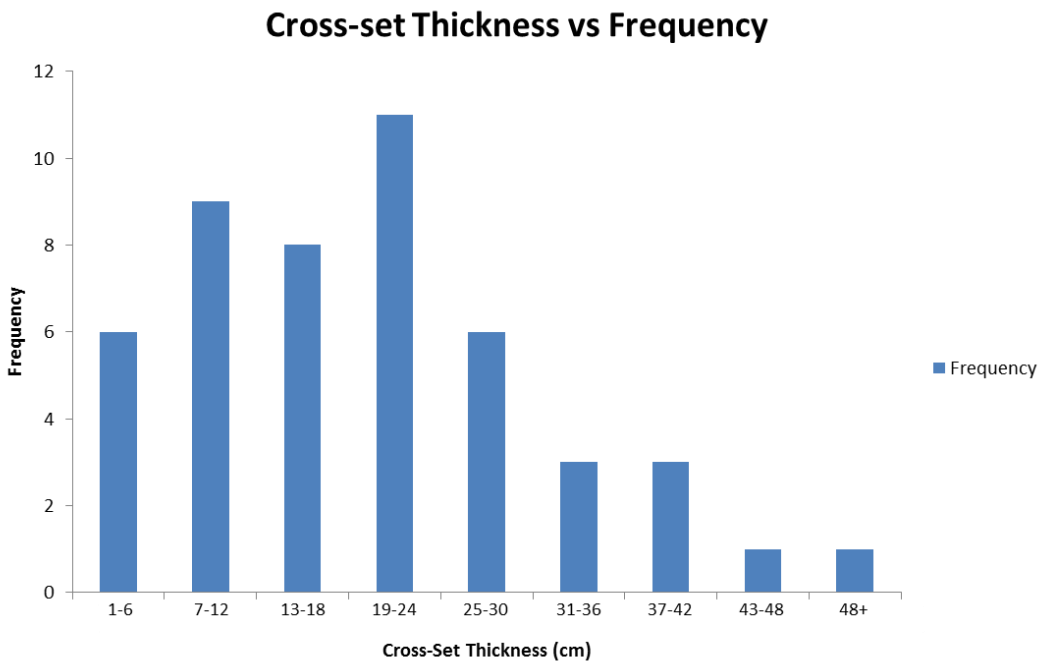

Figure 30. Graph showing cross-set thickness values versus frequency in which they occur for the upper channel belt within Valley 3B. This graph has been modified to show the range of the most frequently occurring cross-set thicknesses.

3.4.2 Paleo-hydraulics of Valley 3A

Lower Channel Belt – Valley 3A

Within the lower channel belt of Valley 3A, 76 cross set thickness were measured and plotted with frequency (fig. 31). The average cross-set thickness for this channel belt is 20.6 centimeters. Thus the resultant average dune height is 61.8 centimeters and paleo-flow depths are between 3.7 and 6.2 meters. However, the cross set thickness occurring most frequently within this channel belt is between 13 to 18 centimeters giving dune heights of 39 to 54 centimeters and a flow depth of 2.3 and 5.4 meters (fig.

32). This range is significantly smaller than those calculated from the average dune height.

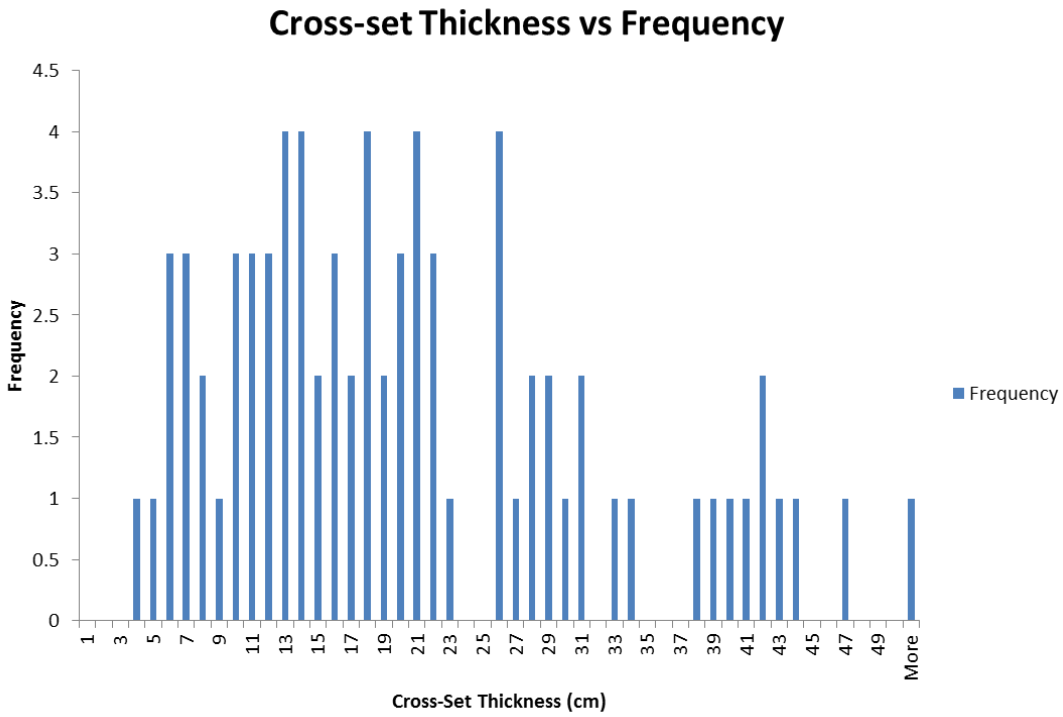

Figure 31. Graph showing cross-set thickness values versus frequency in which they occur for measurements taken within the lower channel belt of Valley 3A.

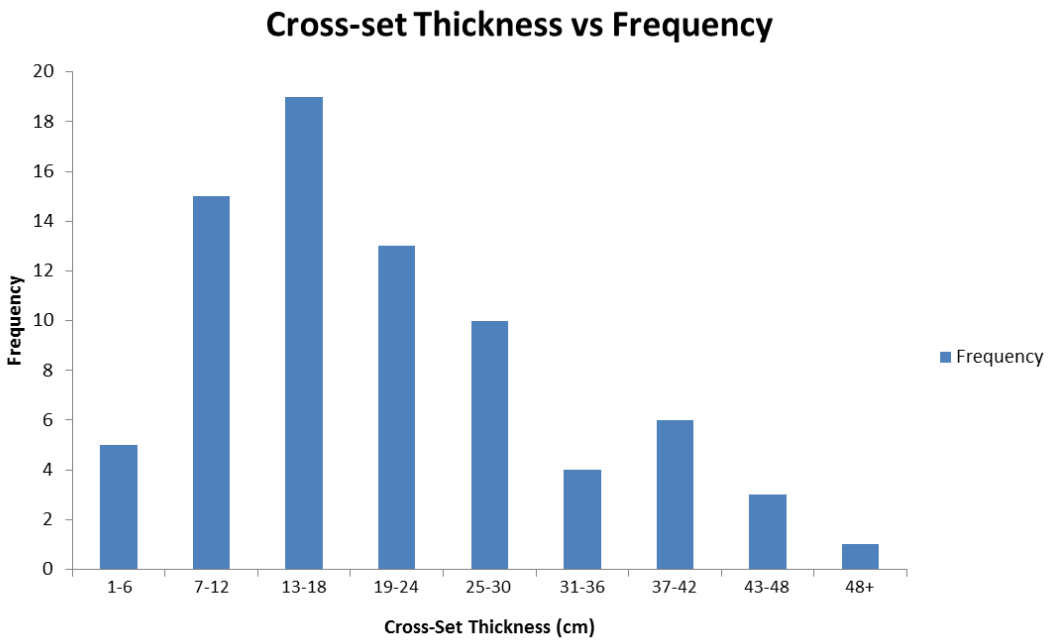

Figure 32. Graph showing cross-set thickness values versus frequency in which they occur for the lower channel belt within Valley 3A. This graph has been modified to show the range of the most frequently occurring cross-set thicknesses.

Middle Channel Belt – Valley 3A

One hundred and thirty-seven total cross-set thickness measurements were taken from the middle channel belt in Valley 3A (fig. 33). These measurement gave an average cross-set thickness of 16.5 centimeters. This gives an average dune height of 49.5 centimeters and paleo-flow depths of 2.9 to 4.9 meters. The most frequent cross-set thickness range proved to be 7 to 12 centimeters, giving an average dune height of 20 to 38 centimeters and a paleo-flow depth of 1.3 to 3.8 meters (fig. 34).

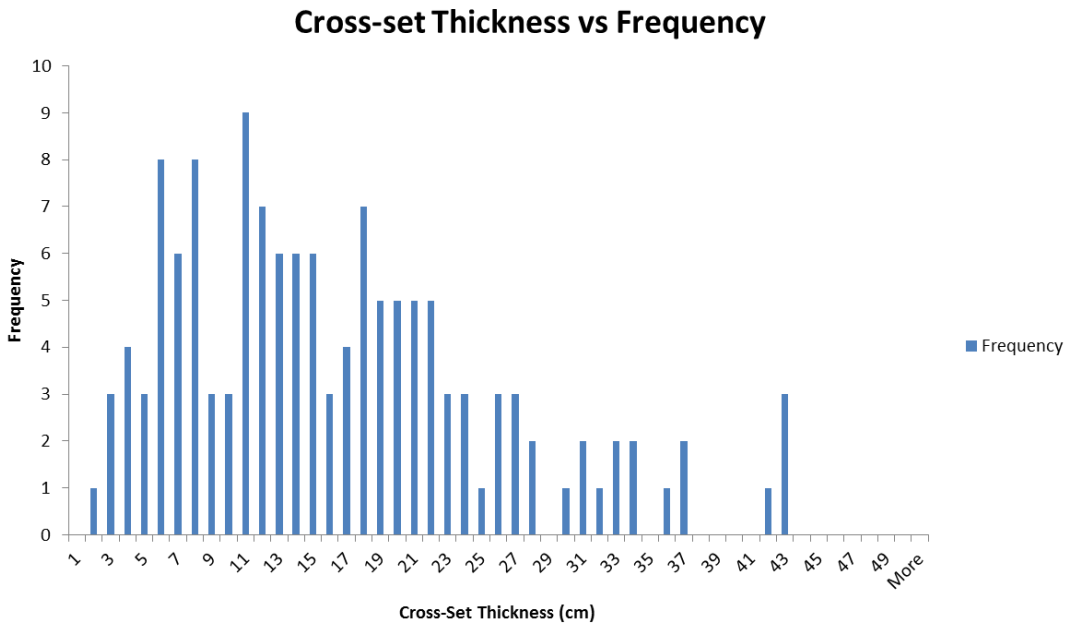

Figure 33. Graph showing cross-set thickness values versus frequency in which they occur for measurements taken within the middle channel belt of Valley 3A.

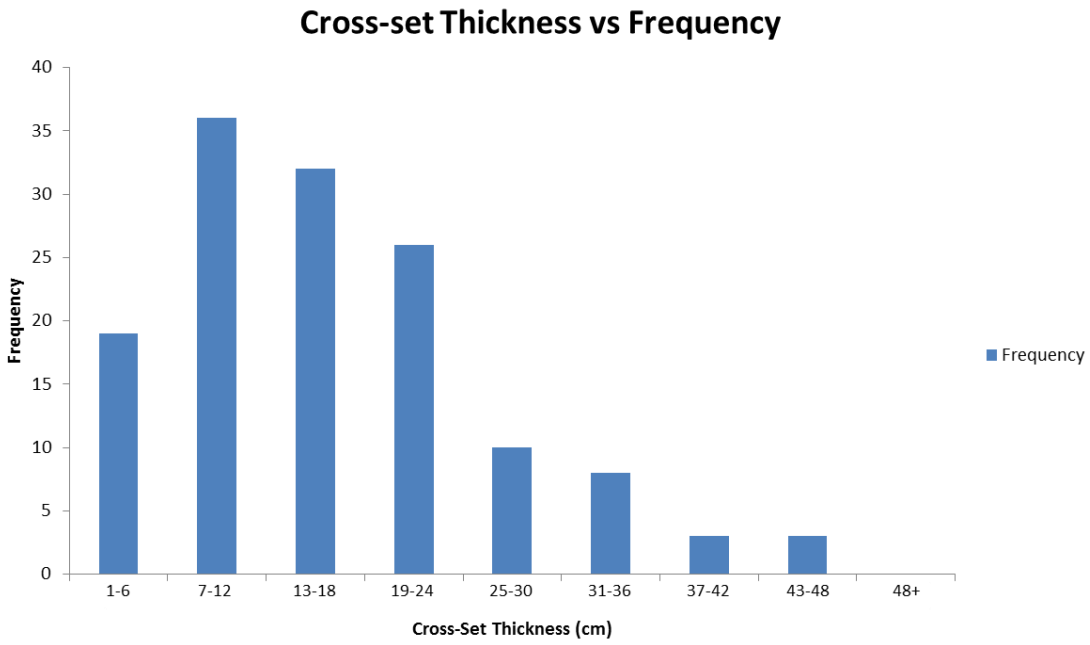

Figure 34. Graph showing cross-set thickness values versus frequency in which they occur for the middle channel belt within Valley 3A. This graph has been modified to show the range of the most frequently occurring cross-set thicknesses.

Upper Channel Belt – Valley 3A

Measurements taken from the uppermost channel belt of Valley 3A proved to be very similar to those taken in middle channel belt. A total of 65 cross-set thicknesses were measured giving an average dune height 16.3 centimeters (fig. 35). This gives a corresponding average dune height of 49 centimeters and a paleo-flow depth of between 2.9 to 4.9 meters. Just like the middle channel belt, the most frequent cross-set thickness range proved to be 7 to 12 centimeters, giving an average dune height of 20 to 38 centimeters and a paleo-flow depth of 1.3 to 3.8 meters (fig. 36).

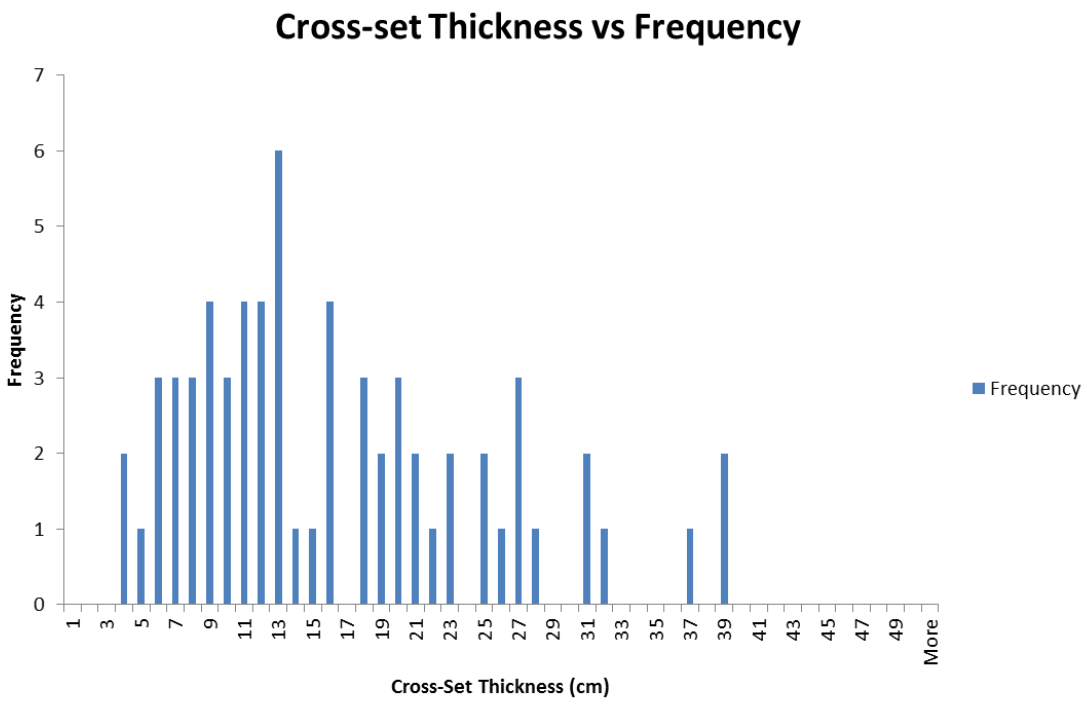

Figure 35. Graph showing cross-set thickness values versus frequency in which they occur for measurements taken within the upper channel belt of Valley 3A.

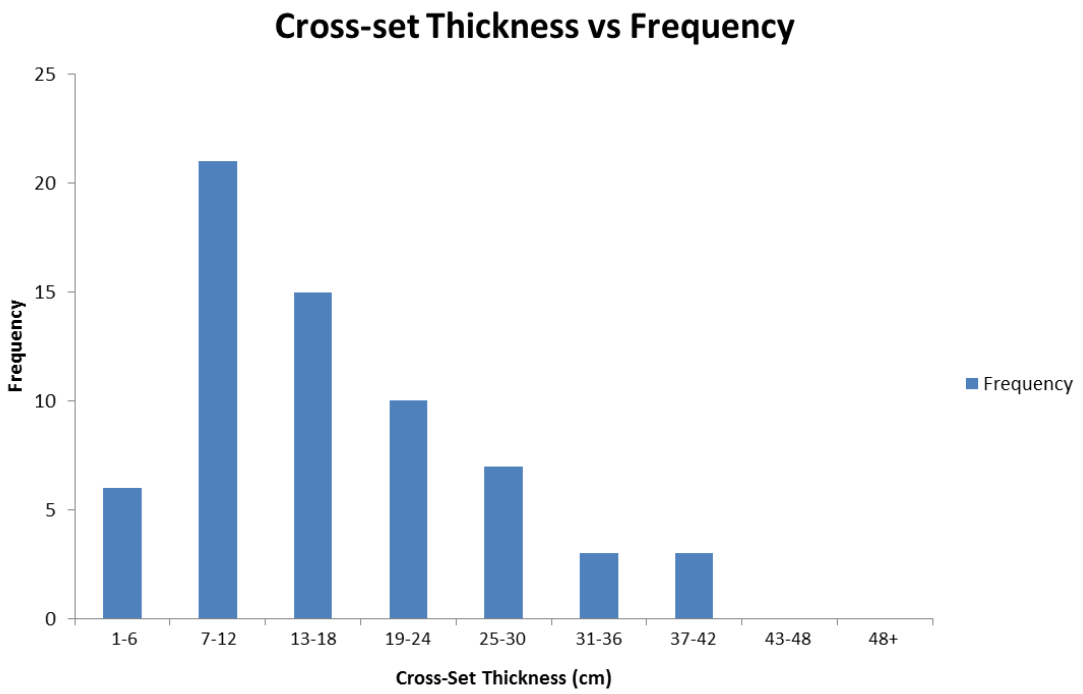

Figure 36. Graph showing cross-set thickness values versus frequency in which they occur for the upper channel belt within Valley 3A. This graph has been modified to show the range of the most frequently occurring cross-set thicknesses.

SECTION 4. DISCUSSION

4.1 Overview

The presence of multiple amalgamated fluvial channels truncating and eroding into marine strata provides strong evidence for a compound incised valley system within Neilson Wash. In areas, there is as much as 14 meters of erosional relief of the basal disconformity while maximum flow depths do not exceed 7.2 meters. The overall erosional relief indicated in regional cross-sections done by Hilton (2013) is

approximately 25 meters. Therefore, the depth of total incision is twice that of the maximum channel depth (fig. 18 & 19). Valley fill deposits onlap and downlap onto the base and sides of the valley wall (fig. 15). Additionally, there exists an abrupt seaward shift of depositional facies across the base of the regionally mappable sequence boundary in which marine sediments are juxtaposed against fluvial strata (fig. 15). Furthermore, there is a well-developed, rooted interfluve that has been interpreted as a paleosol that can be seen from Coal Mine Road before descending into the study area (Campbell, 2013; Hilton 2013). All of these factors satisfy the definition of both Zaitlin (1994) and Posamentier (2001) for an incised valley.

4.2 Coastal Plain Valley Systems and High Frequency Sea-level Fluctuations

Zaitlin et al. (1994) suggested that incised valleys can be divided into two subcategories: Piedmont and Coastal Plain Systems. He defined Coastal Plain Valley Systems as valley systems that can be found within the coastal plain and that are highly susceptible to sea-level fluctuations. Additionally, these systems are composed of generally finer grained more mature sediments. Conversely, Piedmont Valley Systems originate in mountainous settings and generally have coarser grained less mature sediments. The high degree of cut and fill episodes along with evidence for tidal influence and the rounded to sub-rounded sand grains found within the incised valley would indicate that this incised valley system was a Coastal Plain System.

The relative rapid deposition of the IVS along with evidence for tidal influence within the fluvial rocks and the proximity to the coastal plain (parasequence 4) indicate that the valley formed predominantly in response to high frequency sea-level fluctuations. These high frequency, low magnitude events suggest that the valley formed in response to climatic changes associated with Milankovitch Cycles (Zhu et al., 2012).

4.3 General Fluvial Style

Paleocurrent data along with bar accretion directions and a lack of bi-directional downlap in bar deposits from within Valley 3 suggest that the dominant fluvial style found within this valley is that of a meandering stream. Measurements taken from each of the individual channel belts within Valley 3A show that the dominant paleocurrent direction occurred at a high angle to that of bar accretion, which is indicative of a meandering stream (fig. 23, 24, & 26). Shanley and McCabe (1994) and Van Wagoner (1995) have suggested that early, falling stage valley fills should be braided. Previous work done by Li et al. (in press), Hilton (2013) and Campbell (2013) have shown that Valley 3 is a falling stage terrace deposit. Therefore, evidence from Valley 3 is strongly indicative of a meandering river and is contradictory to older, widely accepted sequence stratigraphic models that early valley fills are braided not meandering. This is important because it precludes over-deep incision of early incised valley systems by confluence scours (Best and Ashworth, 1997).

Evidence for a meandering river within Valley 3B, however, is less compelling than that of Valley 3A. Paleocurrent measurements from the lower channel belt occur in nearly the opposite direction from that of bar accretion (fig. 20). This could be indicative of a bi-modal current direction resulting from tidal influence. However, there was no obvious tidal signature within the sedimentary structures of the lower channel belt. These measurements could also be indicative of upstream accretion of the braid bar at the diffluence zone. These anomalous measurements may be misleading as they are probably a consequence of insufficient measurements resulting from poor outcrop exposure. The upper channel belt within Valley 3B also displays an element of downstream accretion (fig. 21). However, this is not entirely indicative of a braided river as point bars within a meandering river can contain a component of upstream and downstream accretion. As a result, we cannot discount that the oldest valley, Valley 3B, formed in response to a braided river as data collected from this valley are insufficient and inconclusive.

4.4 Classification

Incised valley fills can be divided into 3 different segments along their depositional dip profile (Zaitlin et al., 1994; Boyd et al., 2006). These segments (fig. 3) include the marine-dominated segment 1 (seaward outer portion), estuarine-dominated segment 2 (middle portion) and a fluvial dominated segment 3 (landward inner portion)(Li et al., in press). Based on the data collected from outcrop, this IVS most

likely belongs to the segment 2 middle IVS of the idealized incised valley model set forth by Zaitlin et al (1994). Maximum grain sizes found within this terrace deposit are medium-upper, however, extra-formational coarse-grained pebbles can be found within the channel thalweg suggesting direct fluvial derived material. Valley 3 does contain evidence for marine influence within the upper channel belt of Valley 3B. However, the tidally influenced facies accounts for only a minor portion of the entire valley fill. The low degree of tidal reworking along with the presence of extra-formational clasts and the lack of deposits associated with a bayhead delta suggests that this IVS is in the proximal portion of segment 2.

SECTION 5. CONCLUSION

The compound incised valley fill of Valley 3 is that of a coastal plain valley system that formed in response to multiple, high frequency sea-level fluctuations that resulted from climactic changes associated with Milankovitch Cycles. Paleocurrent and bar accretion measurements taken from within the individual channel belts generally showed accretion occurring at high angles to that of the paleocurrent direction. This along with the lack of bilaterally downlapping bar deposits within the IVS suggests that the fluvial style responsible for its formation was meandering. This is contradictory to widely accepted sequence stratigraphic models that early valley fills are braided not meandering. Paleo-flow depths that were calculated based on cross-set thicknesses for Valley 3 indicate a probable channel depths of 3.3 to 5.4 meters. Fill from this IVS would

fall in the segment 2 middle IVS deposits of the simplified IVS model predicted by Zaitlin et al (1994).

REFERENCES

Ardies, G.W., Dalrymple, R.W., and Zaitlin, B.A., 2002, Controls on the geometry of incised valleys in the Basal Quartz unit (Lower Cretaceous), Western Canada Sedimentary Basin: Journal of Sedimentary Research, v. 72, p. 602–618.

Best, J.L., and Ashworth, P.J., 1997, Scour in large braid rivers and the recognition of sequence stratigraphic boundaries: Nature, v. 387, pp. 275 – 277.

Bhattacharya, J.P., 2011, Practical problems in the application of the sequence stratigraphic method and key surfaces: integrating observations from ancient fluvial-deltaic wedges with Quaternary and modeling studies: Sedimentology, v. 58, p. 120-169.

Bhattacharya, J.P., and Tye, R.S., 2004, Searching for modern Ferron analogs and application to subsurface interpretation, *in* T. C. Chidsey, Jr., R. D. Adams, and T. H. Morris, eds., Regional to Wellbore Analog for Fluvial-Deltaic Reservoir Modeling; the Ferron Sandstone of Utah: AAPG Studies in Geology 50, p. 39-57.

Bhattacharya, J.P., and MacEachern, J.A., 2009, Hyperpycnal rivers and prodeltaic shelves in the Cretaceous seaway of North America: Journal of Sedimentary Research, v. 79, pp. 184 – 209.

Blum, M. D., and Aslan, A., 2006, Signatures of climate vs. sea-level change within incised valley-fill successions: Quaternary examples from the Texas Gulf Coast: Sedimentary Geology, v. 190, p. 177–211.

Boyd, R., Dalrymple, R.W., and Zaitlin, B.A., 2006, Estuary and incised valley facies models, *in* Posamentier, H.W., and Walker, R.G., eds., Facies Models Revisited: SEPM, Special Publication 84, p. 171–234.

Bridge, J.S. and Leeder, M.R., 1979, A simulation model of alluvial stratigraphy: Sedimentology, v. 26, p. 617-644.

Bridge, J.S., 2003, Rivers and Floodplains: Forms, Processes, and Sedimentary Record: Blackwell Publishing company, New York, U.S.A.

Campbell, C., 2013, High Frequency sea level fluctuations and complex valley evolution within the Cretaceous Ferron Sandstone, Henry Mountains Basin, Utah, M.S. Thesis, University of Houston.

Catuneanu, O., Willis, A.J. and Miall, A.D., 1998, Temporal significance of sequence boundaries: Sedimentary Geology, v. 121, p. 157–178.

Chidsey, T.C., 2002, Geological and petrophysical characterization of the Ferron Sandstone for 3-D simulation of a fluvial-deltaic reservoir: Utah Geological Survey Miscellaneous Publication 02-6.

Dalrymple, R.W., Boyd, R. and Zaitlin, B.A., 1994, Incised-valley systems; origin and sedimentary sequences: Society for Sedimentary Geology, v. 51, pp. 3 – 10.

D'Souza, D., 2013, Facies architecture, and controls on channel-belt geometry: Cretaceous-Ferron Notom Delta, Utah, U.S.A.: M.S. thesis, University of Houston, Houston.

Gardner, M. H., 1995, Tectonic and eustatic controls on the stratal architecture of mid-Cretaceous stratigraphic sequences, central western interior foreland basin of North America, *in* S. L. Dorobek and G. M. Ross, eds., Stratigraphic Evolution of Foreland Basins: Society for Sedimentary Geology (SEPM) Special Publication No. 52, p. 243–281.

Garrison, J. R. Jr., and van den Bergh, T. C.V., 2004, High-resolution depositional sequence stratigraphy of the upper Ferron Sandstone Last Chance Delta: An application of coal-zone stratigraphy, *in* T. C. Chidsey, Jr., R. D. Adams, and T. H. Morris, eds., Regional to Wellbore Analog for Fluvial-Deltaic Reservoir Modeling; the Ferron Sandstone of Utah: AAPG Studies in Geology 50, p.125-192.

Gibling, M. R., 2006, Width and thickness of fluvial channel bodies and valley fills in the geological record: A literature compilation and classification: Journal of Sedimentary Research, v. 76, p. 731-770.

Hilton, B.D., 2013, Three-D allostratigraphic mapping and facies heterogeneity of a compound, tributary incised valley system, Turonian Ferron Sandstone, Notom Delta, south-central Utah: M.S. thesis, University of Houston, Houston.

Holbrook, J.M., and Bhattacharya, J.P., 2012, Reappraisal of the sequence boundary in time and space: Case and considerations for an SU (subaerial unconformity) that is not a sediment bypass surface, a time barrier, or an unconformity: Earth Science Reviews, v. 113, p. 271 – 302.

Li, W., 2009, Valleys, facies and sequence stratigraphy of the Ferron Notom Delta, Capitol Reef, Utah: Ph.D. dissertation, University of Houston.

Li, W., Bhattacharya, J.P. and Campbell, C., 2010, Temporal evolution of fluvial style in a compound incised-valley fill, Ferron ‘‘Notom Delta’’, Henry Mountains Region, Utah (USA): Journal of Sedimentary Research, v. 80, p. 529–549.

Li, Y. and Bhattacharya, J.P., in press, Facies architecture, branching pattern, and paleodischarge of a lower delta plain distributary channel system in the Cretaceous Ferron Notom Delta, southern Utah, U.S.A.: Sedimentology.

Kvale, E. P., and Archer, A. W., 2007, Paleovalley fills: Trunk vs. tributary: American Association of Petroleum Geologists, Bulletin, v. 72, p. 682-687.

Leclair, S.F. and Bridge, J.S., 2001, Quantitative interpretation of sedimentary structures formed by river dunes: Journal of Sedimentary Research, v. 71, p. 713-716.

Martin, J., Cantelli, A., Paola, C., Blum, M., Wolinsky, M., 2011, Quantitative modeling of the evolution and geometry of incised valleys: Journal of Sedimentary Research, v. 81, p. 64-79.

MacEachern, J.A., Pemberton, S.G., Gingras, M.K., and Bann, K.L., 2010, Ichnology and facies models, *in* James, N.P., and Dalrymple, R.W., eds., Facies Models 4: The Geologic Association of Canada, p. 19 – 58.

Miall, A.D., 1992, Alluvial Deposits, *in* Walker, R. G., and James, N. P., eds., Facies Models: Geological Association of Canada, p. 119-142.

Miall, A.D., 1996, The Geology of Fluvial Deposits: Sedimentary Facies, Basin Analysis and Petroleum Geology: Heidelberg, Springer-Verlag, 582 p.

Miall, A.D., 2010, Alluvial deposits, *in* James, N.P., and Dalrymple, R.W., eds., Facies Models Revisited: SEPM, Special Publication 90, p. 105 – 137.

Peterson, F., and R. T. Ryder, 1975, Cretaceous rocks in the Henry Mountains region, Utah and their relation to neighboring regions, *in* J. E. Fassett and S. A. Wengerd, eds., Canyonlands Country: Four Corners Geological Society Guidebook, 8th Field Conference, p. 167-189.

Peterson, F., Ryer, R.T., and Law, B.E., 1980, Stratigraphy, sedimentology and regional relations of the Cretaceous system in the Henry Mountains region, Utah, *in* Picard, M.D., ed., Henry Mountain Symposium: Utah Geological Association, p. 151 – 170.

Plint, A.G., and Wadsworth, J.A., 2003, Sedimentology and palaeogeomorphology of four large valley systems incising delta plains, Western Canada foreland basin: implications for mid-Cretaceous sea-level changes: Sedimentology, v. 50, p. 1147 – 1186.

Plint, A.G., and Walker, R.G., 1992, Wave- and storm-dominated shallow marine systems: Geological Association of Canada, *in* Walker, R.G., eds., Facies Models, Second Edition, p. 219 – 238.

Plint, A.G., and Wadsworth, J.A., 2006, Delta-plain paleodrainage patterns reflect small-scale fault movement and subtle forebulge uplift: Upper Cretaceous Dunvegan Formation, Western Canada Foreland Basin, *in* Dalrymple, R. W., Leckie, D. A., and Tillman, R. W., eds., Incised Valleys in Time and Space: SEPM, Special Publication 85, p. 219-238.

Plint, A.G., 2010, Wave- and storm-dominated shoreline and shallow-marine systems *in* James, N.P., and Dalrymple, R.W., eds., Facies Model Revisited: SEPM, Special Publication 90, p. 167 – 199.

Posamentier, H.W., 2001, Lowstand alluvial bypass systems: Incised *vs.* unincised: American Association of Petroleum Geologists, Bulletin, v. 85, p. 1771–1793.

Ryer, T.A., and Anderson, P.B., 2004, Facies of the Ferron Sandstone, east-central Utah, *in* Chidsey, T.C., Adams, R.D., and Morris, T.H., eds., The Fluvial-Deltaic Ferron Sandstone: Regional to Wellbore Scale Outcrop Analog Studies and Applications to Reservoir Modelling: AAPG Studies in Geology 50, p. 59 – 78.

Shanley, K.W., and McCabe, P.J., 1994, Perspectives on the sequence stratigraphy of continental strata: American Association of Petroleum Geologists, Bulletin, v. 78, p. 544–568.

Strong, N., and Paola, C., 2008, Valleys that never were: Time surfaces versus stratigraphic surfaces: Journal of Sedimentary Research, v. 78, p. 579-593.

Törnqvist, T. E., Wallinga, J., Busschers, F. S., 2003, Timing of the last sequence boundary in a fluvial setting near the highstand shoreline—Insights from optical dating: Geology, v. 31, p. 279-282.

Van Heijst, M. W. I. M., and Postma, G., 2001, Fluvial response to sea-level changes: a quantitative analogue, experimental approach: Basin Research, v. 13, p. 269 - 292.

Van Wagoner, J.C., Mitchum JR., R.M., Campion, K.M., and Rahmanian, V.D., 1990, Siliciclastic Sequence Stratigraphy in Well Logs, Core, and Outcrops: Concepts for High Resolution Correlation of Time and Facies: American Association of Petroleum Geologists, Methods in Exploration Series, no. 7, 55 pp.

Van Wagoner, J.C., 1995, Sequence stratigraphy and marine to nonmarine facies architecture of foreland basin strata: American Association of Petroleum Geologists Memoir, v. 64, pp. 137 – 223.

Visser, M.J., 1980, Neap-spring cycles reflected in Holocene subtidal large-scale bedform deposits: a preliminary note: Geological Society of America, Bulletin, v. 8, p. 543 – 546.

Wellner, R. W., and Bartek, L. R., 2003, The effect of sea level, climate, and shelf physiography on the development of incised-valley complexes: A modern example from the East China Sea: Journal of Sedimentary Research, v. 73, p. 926–940.

Zaitlin, B.A., Dalrymple, R.W., and Boyd, R., 1994, The stratigraphic organization of incised valley systems associated with relative sea-level change, *in* Dalrymple, R.W., Boyd, R., and Zaitlin, B.A., eds., Incised-Valley Systems: Origin and Sedimentary Sequence: SEPM, Special Publication 51, p. 45–60.

Zhu, Y., 2010, Sequence Stratigraphy and Facies Architecture of the Cretaceous Ferron Notom Delta Complex, South-central Utah, USA: PhD Dissertation, University of Houston, Houston, 144 pp.

Zhu, Y., Bhattacharya, J. P., Li, W., Lapen, T.J., Jicha, B.R. and Singer, B.S., 2012, Milankovitch-scale sequence stratigraphy and stepped forced regressions of the Turonian Ferron Notom deltaic complex, South-Central Utah, U.S.A., Journal of Sedimentary Research, v. 82, p. 723-746.